NAVAL POSTGRADUATE SCHOOL
MONTEREY, CALIFORNIA

THESIS

INTERMETALLIC GROWTH AT THE INTERFACE BETWEEN COPPER AND BISMUTH-TIN SOLDER

by

FRED O. P. VOLLWEILER

September 1993

Thesis Advisor: Professor S. Mitra
Co-Advisor: Professor J. Perkins

Approved for public release; distribution is unlimited.

Unclassified

Security Classification of this page

REPORTS DOCUMENTATION PAGE

1a Report Security Classification UNCLASSIFIED		1b Restrictive Markings	
2a Security Classification Authority		3 Distribution Availability of Report Approved for public release; distribution is unlimited.	
2b Declassification/Downgrading Schedule		5 Monitoring Organization Report Number(s)	
6a Name of Performing Organization Naval Postgraduate School	6b Office Symbol *(If Applicable)* code 034	7a Name of Monitoring Organization Naval Postgraduate School	
6c Address *(city, state, and ZIP code)* *Monterey, CA 93943-5000*		7b Address *(city, state, and ZIP code)* *Monterey, CA 93943-5000*	
8a Name of Funding/ Sponsoring Organization	8b Office Symbol *(If Applicable)*	9 Procurement Instrument Identification Number	
8c Address *(city, state, and ZIP code)*		10 Source of Funding Numbers	
Program Element Number	Project No.	Task	Work Unit Accession No.

11 Title (Include Security Classification)
INTERMETALLIC GROWTH AT THE INTERFACE BETWEEN COPPER AND BISMUTH-TIN SOLDER

12 Personal Author(s) Vollweiler, Fred, O. P.

13a Type of Report Master's Thesis	13b Time Covered From To	14 Date of Report (year, month, day) September 1993	15 Page count 80

16 Supplementary Notation
The views expressed in this thesis are those of the author and do not reflect the official policy or position of the Department of Defense or the U.S. Government.

17 Cosati Codes:	Field	Group	Subgroup

18 Subject Terms *(continue on reverse if necessary and identity by block number)*
Bi-Sn solder, lead free solder, intermetallic growth

19 Abstract *(continue on reverse if necessary and identity by block number)*
Tin-bismuth alloys have been proposed as alterntives to lead containing solders for interconnection and packaging applications. Consequently, the interface between copper metallizations and bismuth-tin solders needs to be evaluated with respect to brittle intermetallic formation. In the binary Bi-Sn alloys both the Cu_6Sn_5 and Cu_3Sn intermetallic phases were found at the Cu/solder interface after exposure at 250°C, 300°C, and 350°C. Bi-Sn-Sb alloys were also studied and in addition to the aforementioned intermetallic compounds Cu-Sb intermetallics were found. Kinetic growth laws have been established for the intermetallics at various temperatures and solder compositions. In addition, bulk samples of the solder were tested in compression in the furnace-cooled and quenched condition. Quenching appeared to result in higher strain rate dependence. Furthermore the tin-rich compositions were more strain rate sensitive than the bismuth-rich composition.

20 Distribution/Availability of Abstract • unclassified/unlimited • same as report • DTIC users	21 Abstract Security Classification UNCLASSIFIED	
22a Name of Responsible Individual S. Mitra	22b Telephone *(Include Area Code)* (408) 970-2014	22c Office Symbol

DD FROM 1473, 84 MAR 83 APR edition may be used until exhausted security classification of this page
All other editions are obsolete Unclassified

Approved for public release; distribution is unlimited

Intermetallic Growth at the Interface Between Copper and Bismuth-Tin Solder

by

Fred O. P. Vollweiler
Lieutenant, United States Navy
B.S., University of Pittsburgh, 1984

Submitted in partial fulfillment of the requirements for the degree of

MASTER OF SCIENCE IN MECHANICAL ENGINEERING

from the

NAVAL POSTGRADUATE SCHOOL
September 1993

Author: 
Fred O. P. Vollweiler

Approved By: 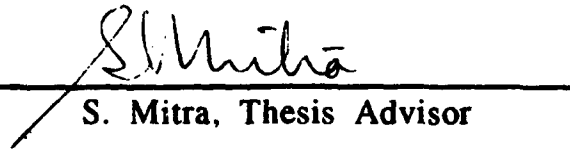
S. Mitra, Thesis Advisor


J. Perkins, Co-Advisor


Matthew D. Kelleher, Chairman
Department of Mechanical Engineering

ABSTRACT

Tin-bismuth alloys have been proposed as alternatives to lead containing solders for interconnection and packaging applications. Consequently, the interface between copper metallizations and bismuth-tin solders needs to be evaluated with respect to brittle intermetallic formation. In the binary Bi-Sn alloys both the Cu_6Sn_5 and Cu_3Sn intermetallic phases were found at the Cu/solder interface after exposure at 250, 300, and 350°C. Bi-Sn-Sb alloys were also studied and in addition to the aforementioned intermetallic compounds, Cu-Sb intermetallics were found. Kinetic growth laws have been established for the intermetallics at various temperatures and solder compositions.

In addition, bulk samples of the solder were tested in compression in the furnace-cooled and quenched condition. Quenching appeared to result in higher strain rate dependence. Furthermore the tin-rich compositions were more strain rate sensitive than the bismuth rich composition.

TABLE OF CONTENTS

I. INTRODUCTION

Joining metals with tin-lead solders is a technology that has been in use since the early bronze age. Ancient cultures used these solders in the manufacture and repair of cooking utensils and metal tools. The Romans used an alloy of lead and tin for sealing their water pipes. Through the ages the process continued to be used primarily by craftsmen in the production of jewelry and artifacts. During the industrial revolution use was greatly expanded with the development of portable torches and electricity to power soldering irons. These tools facilitated the use of solder in applications such as plumbing connections, sealing of food and water containers, and fabrication of heat exchangers such as automobile radiators. [Ref. 1:p. 15]

Soldering of electronics began in the early twentieth century as a means of making electrical connections between copper wires. With the introduction of the silicon chip and the solid state revolution, progress in electronics has been a function of improvement in chip manufacturing and packaging technology. Concurrently, the process of soft soldering as a means of joining electrical components has developed from being strictly an electrical connection between mechanically fastened wires to providing both a mechanical and electrical connection. As such the solder must be capable of withstanding the thermal and mechanical stresses the joint experiences during the service life of the product.

Modern uses of solder can be classified in terms of either structural or electronics applications. The former includes such things as joining together metal tubes or pipes, construction of heat exchangers for air conditioners and automobile radiators, and attachment of metal sheet and plates for cosmetic and light loading applications (an amendment to the safe water drinking act banned the use of lead bearing solders in potable

water plumbing fixtures, and in construction of food processing equipment or containers). [Ref. 1:p. 15]

In the field of electronics, soft soldering has become the most common method of choice for attaching components to printed circuit boards (PCB's), or chip to substrate. In both cases the solder joint functions as the electrical and mechanical attachment medium, making solder joint reliability a critical element in the development of mounting technology, resulting in considerable research into the area of solder and soldering techniques.

A. SOLDERING IN ELECTRONICS

1. Electronic Packaging

Due to the continued decrease in the physical size of electronic components, the role of electronic packaging has taken on an increased importance. A package is essentially the means by which a silicon chip communicates with the outside world. One example, the chip carrier, facilitates the interconnection of the very compact circuits on the chip to the more widely spaced interconnecting pads or holes on the circuit board. The chip carrier also serves to protect the chip from environmental degradation and rugged handling during later stages of the manufacturing process. In addition the package assists in transferring heat away from the chip.

There are several levels of electronic packaging. In the first, the chip, or die, is bonded to the substrate and electrically connected to the output leads of the chip carrier. Typical features of a chip carrier are shown in Figure 1. One method of electrical interconnection that employs solder is flip-chip solder bonding, shown in Figure 2. In this method the solder is deposited onto the substrate in a thin layer and then reflowed into a solder ball or bump at pads on the substrate. Matching pads on the face of the chip are then aligned with those on the substrate, the assembly is heated until the solder spheres begin to

soften and a controlled collapse of the sphere takes place as the solder simultaneously wets both pads [Ref. 2:p. 115].

Chip carriers can be classified based on the type of leads used in the input/output terminals (I/O) emerging from t he carrier as:

1. leaded, intended for pin-in-hole (PIH) mounting to the PCB.
2. leaded, intended for surface mounting on the PCB at solder pads.
3. leadless, in which metallized pads on the chip carrier are soldered to the PCB

Examples of each are shown in Figure 3.

In the second level of packaging the chip carrier is mounted to the PCB. With PIH mounting the chip carrier leads are soldered into holes on the PCB. As can be seen in Figure 3, the mechanical attachment is provided partially by inserting the leads through the holes. The solder joint completes the mechanical connection and provides electrical and thermal continuity between the lead and the through-hole walls [Ref. 3:p. 2]. In surface mount technology (SMT), the solder alone acts as the mechanical and electrical connection. The primary source of mechanical loading in this type of joint is thermal strains resulting from temperature excursions and non-uniformity's within the assembly. These strains must be accommodated by the material connecting these diverse components which is typically a lead based solder [Ref. 4:p. 148].

2. Commonly Used Solders

Table I lists the physical properties of commonly used solder alloys. Of these the lead-tin eutectic (63Sn-37Pb) and near eutectic (60Sn-40Pb) are the most widely used in forming PCB connections. Lead rich solder alloys, such as 95Pb-5Sn, have a higher solidus temperature and are used as part of a step soldering or hierarchical package so that

lower melting point components can subsequently be bonded with eutectic solder without remelting the lead rich joints [Ref. 5:p. 1324].

TABLE I PHYSICAL PROPERTIES OF SOLDER ALLOYS [Ref. 6: p.45]

Alloy Composition	Liquid (°C)	Solidus (°C)	Ultimate Tensile Strength (ksi)	0.2% Yield Strength (ksi)	0.01% Yield Strength (ksi)	Uniform Elongation (%)
42% Sn-58% Bi	138	138	9.71	6.03	3.73	1.3
43% Sn-43% Pb-14% Bi	163	144	5.60	3.60	2.77	2.5
30% In-70% Sn	175	117	4.67	2.54	1.50	2.6
60% In-40% Sn	122	113	1.10	0.67	0.53	5.5
5% In-95% Pb	314	292	3.66	2.01	1.79	33.0
30% In-70% Pb	253	240	4.83	3.58	3.08	15.1
60% In-40% Pb	185	174	4.29	2.89	2.06	10.7
80% Sn-20% Pb	199	183	6.27	4.30	2.85	0.82
63% Sn-37% Pb	183	183	5.13	2.34	1.91	1.38
60% Sn-40% Pb	190	183	4.06	2.06	2.19	5.3
25% Sn-75% Pb	266	183	3.35	2.06	1.94	8.4
10% Sn-90% Pb	302	268	3.53	2.02	1.98	18.3
5% Sn-95% Pb	312	308	3.37	1.93	1.83	26.0
15% Sn-82.5% Pb-2.5% Ag	280	275	3.85	2.40	1.94	12.8
10% Sn-88% Pb-2% Ag	290	268	3.94	2.25	2.02	15.9
5% Sn-93.5% Pb-1.5% Ag	301	296	6.75	3.85	2.40	1.09
1% Sn-97.5% Pb-1.5 Ag	309	309	5.58	4.34	3.36	1.15
96.5% Sn-3.5% Ag	221	221	8.36	7.08	5.39	0.69
95% Sn-5% Ag	240	221	8.09	5.86	3.95	0.84
95% Sn-5% Sb	240	235	8.15	5.53	3.47	1.06
85% Sn-10% Pb-5% Sb	230	188	6.45	3.63	2.62	1.40
5% Sn-85% Pb-10% Sb	255	245	5.57	3.67	2.26	3.50
95% Pb 5% Sb	295	252	3.72	2.45	1.98	13.70

Issues that are important in choosing a solder alloy are melting temperature, wettability, mechanical properties and cost. The popularity of lead based solders is primarily due to their relatively low melting point which is compatible with PCB laminate materials, good wetting characteristics and low cost. However it is a well known fact that lead and lead containing compounds are toxic substances which are harmful to both humans and wildlife if inhaled or ingested in sufficient amounts [Ref. 7]. Several pieces of legislation have been introduced in Congress seeking to regulate the use of lead in a variety of products in order to safeguard public health and the environment. With the number of solder joints produced annually in the United States approaching one trillion [Ref. 2: p. 210], among the items Congress has threatened to ban [Refs. 8-10] are the lead containing

solders which are widely used in the electronics, telecommunications, automotive and aircraft industries. The electronics industry has lobbied vigorously against these bills, noting that the lead used in electronics applications is not accessible for inhalation, ingestion, or other exposure pathways for consumers or users, and that lead exposure in the workplace is already limited and controlled by OSHA. Despite these arguments, industry concerns over possible limits, user taxes, or an outright ban on lead containing solders have spurred considerable interest and research in the development of lead-free alternatives. To be considered as a viable alternative a solder alloy should melt and solidify in the same temperature range as the commonly used tin-lead alloys, have similar mechanical and electrical properties, and have similar wetting characteristics. Table II lists the eutectic tin-lead solder and some of the lead-free solders currently in use and their advantages and disadvantages.

TABLE II PROPERTIES OF LEAD-TIN AND SELECTED EUTECTIC LEAD FREE SOLDERS [Ref. 11:p. 13]

Solder (wt%)	T_m ℃	Advantages	Disadvantages
37Pb-63Sn	183	overall good properties	strctral coarsening; prone to creep
57Bi-43Sn	139	good fluidity	strain rate sensitivity; poor wetting
96.5Sn-3.5Ag	221	good strength, creep resistance	melting point slightly too high
49Sn-51In	120	good wetting	melting point too low; poor ductility; expensive
91Sn-9Zn	199	good strength; abundant	poor corrosion resistance and wetting
95Sn-5Sb	245	creep resistant; mechanically strong	melting point too high
80Au-20Sn	278	creep resistant; corrosion resistant	hard and brittle; melting point too high; expensive

Unfortunately there are at present no known binary alloys which provide all of the aforementioned desirable characteristics. Thus the choice is to utilize an existing binary

lead free binary solder alloy suitable for a specific application, or to attempt to develop a ternary or higher order alloy that could serve as a direct replacement.

One existing lead free binary solder alloy that has found use in certain specialized applications where a low melting point is required, such as in heat sensitive devices, is bismuth-tin. The phase diagram shown in Figure 4 shows that tin and bismuth form a simple eutectic system. Tin melts at 232°C and bismuth at 271°C, both reasonably low temperatures. There is only slight solubility of bismuth in tin in the solid state, and complete miscibility of both of these metals in the liquid state. Generally used in the eutectic composition (42Sn-58B wt%), this alloy is non toxic. However, as Table II shows, the wettability of these solders is poor, and the extremely low melting point (138°C for the eutectic composition) precludes use in high temperature applications, and makes the alloy prone to creep.

This study comprises two parts. The first part is a study of the growth kinetics and morphology of the intermetallics that form at the interface between bismuth-tin solder and a copper substrate during the soldering phase when the solder is still liquid. Two binary compositions, one tin rich and the other bismuth rich, as well as ternary additions of antimony and copper were considered. In the second part, compression tests on the bulk solder material for the two binary compositions, and the ternary alloyed with antimony, were performed. Data from the tests was used to determine the strain rate sensitivity.

II. BACKGROUND

A. SOLDERING BASICS

Metals can be fastened together by a variety of techniques including mechanical fasteners (screws, nuts, bolts, rivets, etc.), adhesive bonding, and metallurgical welding, brazing, and soldering. Of these, metallurgical fastening provides the best thermal and electrical conductive paths. Soldering differs from welding in that only the filler metal (solder) is melted to form the bond [Ref. 3:p. 1]. Solder alloys are characterized as either soft or hard. Soft solders contain elements such as tin, lead indium, cadmium, and bismuth and melt at temperatures below about 350°C. Hard solders contain metals such as gold, zinc, aluminum and silicon, and melt at temperatures above 350°C [Ref. 1:p. 14]. When a bismuth-tin or lead-tin solder is used to join a base metal such as copper, as is the case in many electrical and electronics soldering applications, the interaction between copper and tin is an essential process in forming the metallurgical bond. The joint is achieved by the interfacial reaction between copper and tin, forming intermetallic compounds [Ref. 12:p. 947]. Intermetallic compounds are generally formed between the base elements and the solder by liquid-solid reactions and/or solid state diffusion, either during the soldering operation or during service. Intermetallics have a definite stoichiometric composition, and are characterized by ionic bonds which make them hard and brittle, in comparison to the parent solder alloy [Ref. 3:p. 14]. As such they adversely affect the strength of the solder joint. Figure 5 shows the phase diagrams for both copper-tin and copper-antimony. Intermetallic compounds are designated by greek letters (e.g., η and ε on the Cu-Sn diagram are the intermetallics Cu_6Sn_5 and Cu_3Sn respectively). The function of the lead, or bismuth, in the solder is mainly to lower the melting point and to act as a diluent.

Previous studies using lead-tin solders [Ref. 13] have shown that the thickness of the Cu_6Sn_5 intermetallic which forms at the copper/solder interface plays the greatest role in determining the strength of the bond, with changes in strength closely reflecting changes in thickness of the intermetallic layer. In the study, specimens were tested in shear and in all cases failure initiated in the Cu_6Sn_5 layer, branching into the solder after a period of travel. The extent of failure within the intermetallic layer increased with temperature and resulted from the concomitant increase in thickness of the layer. It has also been shown [Ref. 14: p. 49] that wettability is adversely affected by the intermetallic layer.

From the above it can be seen that an understanding of the growth kinetics and morphology of the intermetallics that form at the interface between the base metal and solder is crucial to predicting the strength and reliability of soldered joints.

B. GROWTH OF INTERMETALLICS AT THE COPPER-TIN INTERFACE

The amount of intermetallic formed at the interface during soldering depends on the solubility of the solder elements in the base metal and on the time and temperature of the soldering. Intermetallics are formed in the body of the solder as it solidifies and as the base metal, dissolved in the molten solder, precipitates out. Subsequent growth of intermetallics during storage and operational service occurs through a solid-state diffusion process. The melting temperature of most solders is relatively low so that in general the operational temperature seen by the solder joint is a relatively high homologous (T_O/T_m) temperature which contributes to the rather rapid solid state reaction of tin and copper to form intemetallic compounds, also resulting in low mechanical strength values and creep resistance.

In general growth of the intermetallic layer with time and temperature can be given by the kinetic equation :

$$x = A\exp(-Q / RT)t^n$$

where x is the thickness of the intermetallic, A and n are constants, t is the reaction time, Q is the activation energy, R is the universal gas constant, and T is the temperature in degrees Kelvin. A linear growth rate, n=1, describes many highly reactive systems (e.g., gold in contact with tin-lead-indium alloys, or copper in tin-indium alloys). Parabolic growth rates, n=0.5, can be used to describe diffusion controlled growth (copper in contact with many tin-lead alloys). Growth rates slower than parabolic describe a growth mechanism controlled in some manner by reactions occurring at the interface between base metal and intermetallic or between intermetallic and solder.

Working with lead-tin solders, Hagstrom and Wild [Ref. 15:p. 271], using direct measurement of the intermetallic layer found growth to be parabolic with time for short times, reaching a limiting value after 10 minutes. Muckett *et al.* [Ref. 16:p. 44] using similar measurements found growth to be linear with time. However, neither of these studies looked at the individual phases within the intermetallic layer. Tu and Thompson [Ref. 12:p. 94], using Raman spectroscopy, found Cu_6Sn_5 to grow linearly with time, and that Cu_3Sn, growing at the expense of the Cu_6Sn_5, grew in a parabolic manner. Parent *et al* . [Ref. 13:p. 2572], also working with lead-tin solder, found that the growth of Cu_6Sn_5 reached a limiting value after 30 minutes and that Cu_3Sn grew linearly with time with no apparent limit to the increase. They also found, in studying the morphology of the intermetallic, that the Cu_6Sn_5 seemed to grow in an irregular manner consisting of a series of sawtooth protrusions becoming more pronounced with time.

Kang and Ramachandran [Ref. 17:p. 422] reported on the growth kinetics of intermetallics at a liquid tin-solid nickel interface. They found growth to occur in 3 stages. For short time and long time reactions growth was seen to be parabolic. For the intermediate stage, growth of the intermetallic slowed due to dissolution in the liquid tin. Two phases of intermetallic were seen, Ni_3Sn_4 and Ni_3Sn_2, with the former phase dominating growth. They also found that after the initial growth of the uniform

intermetallic layer at the Nickel/liquid tin interface, the overall growth of Ni_3Sn_4 was determined by the relative motion of the two interfaces; the Ni_3Sn_4/Sn interface, and the Ni (or Ni_3Sn_2)/Ni_3Sn_4 interface. The motion of the former being due to dissolution of Ni directly from the Ni_3Sn_4 layer because of the slow solid state diffusion of Ni through the Ni_3Sn_4 layer at the reaction temperatures considered (300, 400 and 500°C). The motion of the dissolving interface slowed down as the liquid Sn became saturated with Ni. The motion of the second interface was affected by the presence of the second or third intermetallic phases. The kinetic data showed that the motion of both interfaces was more or less balanced during the intermediate stage, resulting in the slow growth observed. It was found that the balance was disturbed when the dissolution of the intermetallics decreased, resulting in the resumption of parabolic growth at longer times. In terms of morphology they found planar growth to occur for short times ($t < 30$ sec) with faceting occurring during longer ($t > 30$ min.) reactions.

C. MECHANICAL PROPERTIES OF BISMUTH-TIN SOLDER

As previously noted, in modern soldering of electronic components the solder acts as both an electrical and mechanical connection throughout the different levels of packaging in the device. Increased miniaturization and high circuit speeds have resulted in harsh operating conditions for the solder joint, and as a result, joint reliability problems. Since solders sit at the interface between dissimilar metals, the most important load geometry is generally shear which is imposed by mismatched thermal expansion characteristics of the diverse materials joined by the solder, and cyclic temperature fluctuations encountered during service. These events cause thermal fatigue in the constrained solder, particularly in surface mounted leadless components. Since the solder is mechanically soft and is used at a high homologous temperature, deformation is introduced by plasticity and creep during the strain cycles. [Ref. 6:p. 225]

The microstructure of a material, dictated by its processing history, determines the mechanical properties that it will exhibit when subjected to such environmental factors as temperature, and stress. For solder alloys of a given composition, which are used in the as cast state, the chief variable in terms of processing is the cooling rate. Cooling rates of thick joints are relatively slow, while thin joints may experience rapid cooling. There has been relatively little fundamental research in the mechanical metallurgy of bismuth-tin solders. The eutectic solders that have been studied tend to have well developed eutectic microstructures regardless of cooling rate.

In terms of mechanical properties, Morris *et al* . [Ref. 18:p. 27] found that when bismuth-tin solder is strained in shear at moderate strain rates the solder hardens to a maximum, then softens dramatically until failure, with stress-strain behavior governed by high temperature creep as expected due to the high homologous temperature. Tomlinson and Collier [Ref. 19] found that a cast eutectic bismuth-tin solder alloy failed at an elongation of 16.6% indicating relatively low ductility and possibly poor thermal fatigue resistance. Pattanaik and Raman [Ref. 20], however, found that the tensile properties of eutectic bismuth-tin solders depend heavily on strain rate, and that at low strain rates the solder is relatively ductile, an important finding given that strain rates during thermal fatigue are generally low [Ref. 21:p. 28]. It must be remembered, however, that the strength of a bismuth-tin/copper solder joint depends considerably on the extent to which intermetallic compounds form at the base metal/solder interface, since, as suggested by Parent *et al*. [Ref. 13:p. 2572], crack initiation generally takes place in the intermetallic layer, rather than the bulk solder.

III. EXPERIMENTAL PROCEDURES

A. INTERMETALLIC FORMATION

1. Materials

Experiments were divided into two main categories: (i) examination of the growth kinetics and surface morphology of the intermetallic compounds formed at the copper-solder interface, and, (ii) compression tests on the bulk solder material. Four compositions of solder were studied in the intermetallic growth experiments. These were: 70Bi-30Sn, 30Bi-70Sn, 68Bi-29Sn-3Sb, and 37Bi-58Sn-5Cu (wt%). The two binary compositions and the ternary (Bi-Sn-Sb) alloy were subjected to mechanical testing.

Preparation of the bulk solder material was identical for both sets of experiments. For the binary compositions tin shot and bismuth rods of 99.98% purity were combined in the proper ratio and melted in a ceramic crucible in the presence of argon gas to prevent oxidation. The ternary alloys were prepared in the lab utilizing antimony powder (100 mesh, 99.5% purity), and copper powder (40 mesh, 99.5% purity) respectively in addition to the aforementioned tin and bismuth. The antimony powder was first melted, then allowed to cool in air and broken into small pieces prior to addition to the molten tin-bismuth solder. The mixture temperature was brought to $400^{\circ}C \pm 2^{\circ}C$ and held at that temperature for two hours under an inert atmosphere to allow complete dissolution. During this time it was agitated frequently to ensure complete mixing. For the sample containing copper, the copper powder was placed in a 6 molar HCl solution to remove the oxide layer prior to its addition to the molten tin-bismuth solder. Again the mixture temperature was brought to $400^{\circ}C$ for two hours, agitating frequently to ensure complete mixing.

2. Method

To study the growth of the intermetallic compounds formed at the copper-solder interface, copper wires were immersed in a molten solder bath. The copper wire specimens were approximately 7 cm long and 0.8 mm in diameter with a purity of 99.90%. To ensure good wetting, the specimens were sanded lightly using 600 grit emery paper to remove the oxide layer, degreased for 30 seconds in a 6 molar hydrochloric acid solvent, rinsed in distilled water, and air dried prior to immersion. Approximately 50 grams of solder were held in a ceramic crucible in the presence of an inert gas (argon). The solder was heated in a resistance heated furnace and the temperature recorded with a thermocouple. The temperature was maintained at $\pm 4^{\circ}C$ during the immersion experiments, at levels of 250°C, 300°C, and 350°C for the binary compositions and 300°C, 350°C, and 400°C for the two ternary compositions. Immersion times varied from 30 seconds to a maximum of 10 minutes. Specimens were quenched in water immediately after removal from the solder bath. After quenching small segments (approximately 3-4 mm in length) were cut from the tips of the copper wires to be used for viewing the surface morphology of the individual specimens, and in x-ray diffraction tests. The remainder of the specimens were mounted in a matrix of solder using an alumina crucible as a mold. For each composition and temperature five copper wire specimens (immersed for different lengths of time) were mounted by placing them into the crucible, pouring liquid solder around them, and quenching immediately in water. Specimen preparation for Scanning Electron Microscope (SEM) viewing consisted of wet grinding on progressively finer emery paper down to 600 grit, and polishing on 6um and finally 1um diamond paste polishing wheels. Specimens were cleaned using ethanol and dried with warm air [Ref. 22:p. 400]. This method of polishing prevented steps from forming on the surface of the specimens due to the differences in hardness between the copper, tin, and any intermetallics. Specimens were then placed in the scanning electron microscope and viewed in cross-section (Figure 6) so

that the intermetallic formed at the copper-solder interface could be measured. It was found that backscattered electron imaging provided the most effective means for viewing the intermetallic layer. To determine the thickness of the generally uneven layer 20-30 measurements were made along the copper-solder interface around the entire circumference of the wire using the micrometer built into the SEM. The reported thickness values are the maximum, minimum, and mean of these measurements.

To examine the surface morphology of the intermetallic formed on the copper wires the overlying coating of solder was etched off with a solution of 10 parts sodium hydroxide (NaOH) plus 7 parts orthonitrophenol ($C_6H_5NO_3$) in 1 liter of distilled water. The specimen was placed in the solution at a temperature of 75°C and ultrasonically agitated [Ref. 23:p. 158]. After complete removal of the tin, indicated by a uniform matte grey appearance, the specimens were removed, washed in distilled water, and dried using acetone. This method proved very effective in stripping off the outer layer of tin, and backscattered electron imaging proved to be the most effective method of examining the surface morphology of the intermetallic layer.

For X-ray diffraction analysis of the intermetallic compounds the specimens were prepared in the same manner as described above (i.e., for viewing the surface morphology). The surface of the sample was scanned using CuKα radiation in a Phillips diffractometer with model 3100 X-ray generator and PW1710 diffractometer control unit, using ADP software. Analysis of the recorded scans was performed to identify the intermetallic phases present as a function of time, temperature, and composition.

B. MECHANICAL TESTING

1. Method

Compression tests were performed on three of the four bulk solder alloys that were melted and cast using two different cooling rates: (i) quenched and (ii) furnace cooled. The compositions tested were: tin rich (30Bi-70Sn), bismuth rich (70Bi-30Sn), and bismuth rich alloyed with antimony (68Bi-29Sn-3Sb).

Approximately 50 grams of the bulk solder for each alloy was melted in a ceramic crucible in the presence of an inert gas (argon) to prevent oxidation. Temperature of the melt was 300°C for the binary compositions and 350°C for the ternary. The molten solder was then poured into cylindrical stainless steel molds measuring 6.5 mm in height and approximately 6.5 mm in diameter. After a dwell of 30 seconds the mold was quenched in room temperature water from bottom to top. Half of the samples were then placed in a freezer at 0°C for storage until testing. The other half of the samples were placed back into the furnace, reheated to the aforementioned temperature (300°C or 350°C) and allowed to cool slowly to room temperature. These samples were then also placed into a freezer for storage until testing was begun. In preparation for the compression tests the surfaces of the specimens were lightly sanded on 400 grit emery paper to ensure proper alignment at the platen surface/sample interface.

Compression tests were performed on an Instron model 4505 machine equipped with a model 4500 advanced panel incorporating a standard computer interface as a means of system control, data acquisition, and processing. A 10 KN calibrated load cell was used in conjunction with series IX Automated Materials Testing System version 5.24 software. Tests were performed on 5 samples per alloy for each of the two cooling rates, at crosshead speeds of 0.05, 0.1, 0.5, 1.0, and 5.0 mm/min.

The stress vs. strain curves (engineering values) generated from the Instron data were plotted to obtain values of flow stress at 5, 10, and 20 percent strain for each of the samples tested. Strain rates were computed from the relation:

$$\varepsilon = 1/L(dL/dt)$$

where dL/dt is the crosshead speed, and L is the initial sample height. A log-log plot of the flow stress values vs. the strain rate was then constructed to determine the strain rate sensitivity as a function of cooling rate for the different compositions. Stress and strain rate are related according to the following expression:

$$\sigma = K\varepsilon^m$$

where m is the strain rate sensitivity. Taking the natural log of both sides:

$$\ln\sigma = \ln K + m(\ln\varepsilon)$$

yields a value for 'm' from a $\ln\sigma$-$\ln\varepsilon$ plot.

Due to the fact that room temperature is a relatively high homologous temperature for these alloys and plastic deformation was present from the start of the test, no true initial straight line portion existed for the stress/strain curve. Young's modulus was thus not computed.

In addition to the mechanical testing of the bulk solder, microstructural comparisons of as cast material and post compression test samples were made in the SEM. Samples were prepared for the SEM in the same manner as previously described for viewing the intermetallic layer.

IV EXPERIMENTAL RESULTS AND DISCUSSION

A. INTERMETALLIC FORMATION

1. Tin Rich (30Bi-70Sn wt%)

Representative micrographs of the cross sections of the intermetallic grown on copper wire after immersion in a tin-rich solder bath at 300°C for 2 minutes, 5 minutes, and 10 minutes are shown in Figures 7 (a-c) respectively. Growth of the intermetallic layer can clearly be seen as time progresses. The initial layer of Cu_6Sn_5 resembles a series of sawtooth protrusions. With time a layer of Cu_3Sn grows at the Cu/intermetallic interface at the expense of the Cu_6Sn_5. These two layers of intermetallic between the copper and the solder can be seen in Figure 8 where the cross section, after immersion at 350°C for 5 minutes appears darker near the copper. This signifies less tin, as these are backscattered images. This was also checked by energy dispersive X-ray spectroscopy (EDXS). Similar growth patterns have been found in previous studies [Refs. 5,13].

Figure 9 shows the surface morphology of the intermetallic on copper grown in the tin-rich solder. The micrographs show that growth of the intermetallic layer becomes more faceted at higher temperatures and longer immersion times. Previous work [Ref. 13] has identified similar behavior in lead-tin solders where it was found that there was an apparent limit to the growth of the intermetallic layer for times greater than 30 minutes. This limit seemed to be the result of competition between the motion of the Cu_3Sn/Cu_6Sn_5 boundary and some dissolution of the Cu_6Sn_5 into the liquid solder, with dissolution being indicated by the observed faceting.

Analysis of x-ray diffraction scans of the intermetallic layers revealed primarily Cu_6Sn_5 for immersion times less than 3 minutes. For longer immersion times and

temperatures above 300°C, ε (Cu_3Sn) was also found. Due to the extremely short times and thin layers, the exact thickness of the Cu_3Sn and Cu_6Sn_5 layers could not be determined with any accuracy. However, it is likely that the Cu_3Sn layer formed at the expense of the Cu_6Sn_5, as suggested by Figure 7.

Average thicknesses measured for of the intermetallic layer at each of the three temperatures considered are shown in graphical form in Figure 10 and summarized in Table III.

TABLE III INTERMETALLIC THICKNESS FORMED ON CU IN 30BI-70SN SOLDER

T (°C)	X 1/2min (um)	X 1min (um)	X 3min (um)	X 5min (um)	X 10min (um)	Slope of t^1/2
250	.38	0.51	0.92	1.03	1.70	0.07
300	0.85	1.27	2.07	2.47	3.90	0.16
350	0.95	1.33	2.04	3.08	4.05	0.17

The growth rate for all three cases was seen to be parabolic, suggesting that the growth is controlled by the long range diffusion of one of the constituents (i.e., Cu or Sn). The greatest change in thickness occurs between 250°C and 300°C. Ref. 13 observed similar growth kinetics in experiments performed using lead-tin solder, where the two intermetallic phases were examined separately in terms of growth. It was noted in that study [Ref. 13] that in addition to the increase in kinetics resulting from increased diffusion at higher temperatures, there is an increase in the solubility of copper in tin between 250°C and 300°C which may delay the retarding action of saturation in the melt, and at least partially account for the increased thickness at higher temperatures. Two competing mechanisms can be identified: (i) the growth of the Cu_3Sn layer due to consumption of Cu at the substrate side, and (ii) the dissolution of Cu_6Sn_5 at the liquid tin side. Dissolution can result in the morphology shown in Figure 9c. In the present study, however, the increase in the rate of growth was smaller between 300°C and 350°C as compared to that between 250°C and 300°C. This may indicate that a limiting value of the growth rate may exist.

These growth rates appear as kinetic constants in the equation governing diffusion controlled growth:

$$x = Kt^{1/2}$$

where x = thickness, t = immersion time and K is the kinetic constant.

2. Bismuth rich (70Bi-30Sn wt%)

Figure 11 shows representative micrographs of the intermetallic layer found in the bismuth rich samples. Numerous small pockets of bismuth at the Cu/intermetallic interface can be seen in Figure 11b. This was noted in all of the bismuth rich samples at immersion times greater than 5 minutes and solder bath temperatures of 300°C or greater.

Analysis of X-ray diffraction scans on the surface of the intermetallic, such as that shown in Figure 12, revealed large amounts of bismuth (due to incomplete removal by the nitrophenol-NaOH solution), copper, and Cu_6Sn_5, with perhaps a small amount of Cu_3Sn. EDX microprobe analysis of samples with immersion times greater than 3 minutes confirmed that a layer of Cu_3Sn was located at the Cu/solder interface, in a similar fashion to that seen in the tin rich composition. Figure 13 shows the results of two of the EDX analyses taken at different locations within the intermetallic layer of a sample immersed for 5min at 350°C. Data in Figure 13a was taken with the probe placed near the Cu/intermetallic interface (Cu_3Sn), while that in Figure 13b was taken with the probe near the intermetallic/liquid solder interface.

Results of the intermetallic growth measurements for the bismuth rich samples are shown in Figure 14 and summarized in Table IV. The data appear to fit a straight line when plotted as x versus $t^{1/3}$ and seem to indicate that growth in this case is controlled by some type of interfacial reaction rather than by the long range diffusion of copper or tin.

At 300°C the recorded thickness measurements for each of the times considered are lower than those achieved at 250°C. The reasons for this are not fully understood, however, as can be seen in Figure 15 the surface morphology of the layer after immersion

for 1 minute at 250°C already shows features indicative of dissolution of the intermetallic. At 300°C therefore, it is likely that dissolution exceeds the rate of growth and the overall thickness of the layer is lower than that at 250°C.

TABLE IV INTERMETALLIC THICKNESS FORMED ON CU IN 70BI-30SN SOLDER

T (°C)	X 1/2min (um)	X 1min (um)	X 3min (um)	X 5min (um)	X 10min (um)	Slope t^1/3
250	1.31	1.45	1.99	2.38	2.82	0.37
300	1.00	1.35	1.81	2.02	2.71	0.34
350	1.78	2.31	2.54	2.96	3.25	0.38

As the temperature of the melt is further increased to 350°C, it can be seen that the thickness and growth rate are higher than at either of the two lower temperatures. However, there also appears to be a period of rapid initial growth in the first 30 seconds which is not seen at the lower temperatures. Growth then levels off at a rate similar to that achieved at 250°C.

3. Bismuth rich alloyed with antimony (68Bi-29Sn-3Sb wt%)

In addition to the copper-tin intermetallics found previously in the binary compositions, the ternary addition of antimony results in the formation of copper-antimony intermetallic compounds. Figure 16 shows representative micrographs taken during thickness measurements on the cross sections of copper wires immersed in the solder bath. Measurements were made at temperatures of 300°C, 350°C, and 400°C. As in the bismuth rich binary composition (at high temperatures and longer times) the presence of bismuth at the Cu/intermetallic interface was noted in virtually all of the samples immersed in the composition alloyed with antimony, the effect becoming more pronounced for longer immersion times. In Figure 16a, EDX microprobe analysis revealed growth of Cu_3Sn close to the Cu/intermetallic interface, with the η phase ($Cu_{3.3}Sb$) of the copper-antimony intermetallic at the intermetallic/solder interface. Other regions revealed only Cu_6Sn_5, with no Sb containing intermetallic compound. Figures 17 and 18 show several SEM

micrographs of the surface morphology of the intermetallic layer. Figure 17a shows the η phase (copper-antimony intermetallic) after an immersion time of 5 minutes at 300°C. The morphology appears faceted with some hexagonal shapes and some larger platelets. Figure 17b shows a layer of Cu_6Sn_5 growing beneath a layer of bismuth which remained after etching with the nitrophenol/NaOH solution. No Sb was found in this layer by EDX microprobe analysis. Figure 18 shows the Cu-Sb intermetallic after immersion of the copper wire at the highest temperature (400°C) and the longest time (10 minutes) considered. The micrograph reveals a highly compacted layer with the platelets and hexagonal shapes barely distinguishable.

Figure 19 depicts graphically the results of the thickness measurements. These results are also summarized in Table V.

TABLE V INTERMETALLIC THICKNESS FORMED ON CU IN 68BI-29SN-3SB SOLDER

T (° C)	X 1/2min (um)	X 1min (um)	X 3min (um)	X 5min (um)	X 10min (um)	Slope t^1/3
300	1.53	1.80	2.00	2.17	2.46	0.19
350	2.13	2.82	2.91	3.49	3.68	0.31
400	2.13	2.69	2.39	2.72	2.69	-0.01

There appears to be an initial period of rapid growth during the first 1/2 minute at 300°C and 350°C, and 1min at 400°C, similar to what was seen in the bismuth rich binary composition at 350°C. This fast initial growth then appears to be followed by some type of interfacially controlled growth at a much slower rate. At 300°C and 350°C there is an increase in thickness with both temperature and time, however at 400°C the thickness of the intermetallic layer is less than at either of the two lower temperatures for all times considered. In addition, at 400°C growth appears to virtually cease after 1 minute and may in fact actually decrease with time, indicating that the rate at which the intermetallic is dissolving at the liquid solder interface is at least equal to the rate at which the Cu/intermetallic interface is growing.

Although it is not fully understood why some regions grow as Cu-Sb intermetallics and some as the Cu-Sn intermetallic, the presence of both, in all samples, was confirmed by X-ray scans (e.g., Figure 20) as well as EDX microprobe analysis during thickness measurements.

4. Tin rich alloyed with copper (37Bi-58Sn-5Cu wt%)

Figure 21 shows representative SEM micrographs of cross sections of copper wire after immersion in a 37Bi-58Sn-5Cu liquid solder bath at 300°C, 350°C, and 400°C. The presence of small voids clustered at the Cu/intermetallic interface and scattered throughout the layer can clearly be seen at 300°C and 350°C. These voids appeared in all Cu alloyed samples at these temperatures for immersion times greater than 3 minutes. At 400°C (Figure 21c) the voids are absent, as was the case for all immersion times at this temperature. These voids may be due to the Kirkendall effect, resulting from an inequality of the diffusion fluxes during intermetallic growth causing porosity to develop [Ref. 24:p. 147]. This porosity would probably tend to further weaken the already brittle Cu_6Sn_5 which forms adjacent to the copper wire.

Figure 22 shows additional SEM micrographs of cross sections of copper wire after immersion in a melt at 350°C. After 3 minutes (Figure 22a) there are virtually no voids present, however some unusually large sections of planar growth as well as a long dendrite of Cu_6Sn_5 can be seen in this micrograph. These were also noted at longer immersion times for both 300°C and 350°C melt temperatures. Both the η (Cu_6Sn_5) and ε (Cu_3Sn) phases of intermetallic can be seen in Figure 22b with ε being the darker region at the Cu/intermetallic interface and η the lighter region immediately below the solder. This was verified using EDX analysis. Numerous voids are also noted in this micrograph. A large increase in the number of voids is seen in Figure 22c, taken after a 10 minute immersion at 350°C.

Analysis of X-ray diffraction scans of the surface of the copper wires (Figure 23) shows that, at shorter times the intermetallic formed was primarily composed of the η phase (Figure 23a). For longer immersion times (Figure 23b) the presence of both ε and η phases was confirmed.

Examination of the surface morphology of the intermetallics revealed faceted growth even at very short immersion times and low temperatures (Figure 24). In Figure 24a, which shows the morphology of the intermetallic on copper wire immersed at 300°C for 1/2 minute faceted particles appear to have nucleated on the grinding marks left after removal of the surface oxide from the copper wire prior to immersion. At 350°C after a 5 minute immersion in the solder bath (Figure 24b) the morphology of the intermetallic layer appears very different from the layer that forms at 400°C after 10 minutes (Figure 24c). It is interesting to note that the immersion time and temperature of 10 minutes at 400°C corresponds to a marked reduction in the thickness of the intermetallic layer.

Average results for the thickness measurements of the intermetallic layer are shown graphically in Figure 25 and summarized in Table VI.

TABLE VI INTERMETALLIC THICKNESS FORMED ON CU IN 37BI-58SN-5CU SOLDER

T (°C)	X 1/2min (um)	X 1min (um)	X 3min (um)	X 5min (um)	X 10min (um)	Slope of t^1/3
300	2.38	2.83	3.25	3.82	5.66	0.55
350	2.33	2.88	3.15	3.81	4.10	0.34
400	1.96	1.95	2.02	2.09	1.67	-0.04

As in the ternary composition alloyed with antimony, the initial growth rate is relatively high for all three temperatures. At 300°C there is only a modest reduction from the initial fast growth at longer times, and in fact growth appears to accelerate between 5 and 10 minutes. At 350°C the initial growth rate is faster than that at 300°C, while the growth rate after the first 1/2 minute is slower. At a melt temperature of 400°C the growth in the first

1/2 minute appears similar to that at 350°C. With time the growth rate appears to become negative and a reduction in the thickness of the intermetallic layer is noted.

5. Summary of results

Table VII presents a summary of the thickness measurements for all compositions considered in this study. Analysis of the data shows that addition of Sb to the Bi rich (70Bi-30Sn) composition results in an overall increase in the intermetallic thickness at 300°C and 350°C, although the kinetic constant appears smaller in the presence of Sb. This is attributed to the initial rapid growth seen in the presence of Sb. At 400°C, the Sb containing solder results in a decrease in the layer thickness with time.

TABLE VII SUMMARY OF THICKNESS MEASUREMENTS

SAMPLE (comp)	T (°C)	X 1/2 (um)	X 1min (um)	X 3min (um)	X 5min (um)	X 10min (um)	Slope t^1/2	Slope t^1/3
30Bi-70Sn	250	.38	0.51	0.92	1.03	1.70	0.07	-
	300	0.85	1.27	2.07	2.47	3.90	0.16	-
	350	0.95	1.33	2.04	3.08	4.05	0.17	-
70Bi-30Sn	250	1.31	1.45	1.99	2.38	2.82	-	0.37
	300	1.00	1.35	1.81	2.02	2.71	-	0.34
	350	1.78	2.31	2.54	2.96	3.25	-	0.38
68Bi-29Sn-3Sb	300	1.53	1.80	2.00	2.17	2.46	-	0.19
	350	2.13	2.82	2.91	3.49	3.68	-	0.31
	400	2.13	2.69	2.39	2.72	2.69	-	-0.01
37Bi-58Sn-5Cu	300	2.38	2.83	3.25	3.82	5.66	-	0.55
	350	2.33	2.88	3.15	3.81	4.10	-	0.34
	400	1.96	1.95	2.02	2.09	1.67	-	-0.04

The addition of Cu to the solder results in a departure from the diffusion controlled growth seen with the 30Bi-70Sn solder. Furthermore, with Cu in the solder, the kinetic constant appears negative at 400°C as dissolution of the intermetallic occurs.

B. MECHANICAL TESTING

Bulk solder specimens of the two binary compositions, and the ternary alloyed with antimony, were subjected to mechanical testing in both the furnace cooled and quenched conditions. The specimens were compressed to approximately one half their original height at several strain rates in the range of 0.000013 to 0.013 /sec (.005 to 5.0 mm/min crosshead speed with a specimen height of 6.5 mm). Force-displacement curves collected in the Instron tester were converted to stress-strain data. Representative stress-strain plots are shown in Figure 26. From the stress-strain plots the flow stress values at 5, 10, and 20% strain were determined for each strain rate. Results are given in tables VIII (5%), IX (10%), and X (20%) as a function of composition and cooling rate. These results show that the flow stress at 5 and 10% is consistently lower for the quenched samples until a strain rate of .00256/sec or greater is reached. At faster strain rates the trend reverses and the quenched samples for all 3 compositions are seen to be stronger. At 20% strain the slow cooled samples exhibit higher flow stress values regardless of the strain rate for the two binary compositions, however, in the sample alloyed with antimony the quenched specimen has a higher flow stress value for the fastest strain rate. In terms of composition, at 5 and 10% strain for the slow cooled samples, as expected, the tin rich sample achieved consistently higher strengths than either of the bismuth rich alloys, although the ternary alloy has comparable strengths at low strain rates ($\leq$ 0.00256/sec). At 20% strain the tin rich binary and bismuth rich ternary alloys are comparable at all strain rates, and both appear stronger than the bismuth rich binary composition. For the quenched samples the ternary alloy had the highest flow stress values at 5 and 10% strain for low strain rates, while the tin rich binary composition was greater at faster strain rates.

TABLE VIII FLOW STRESS AT 5% STRAIN

SAMPLE	5% Flow Stress (MPa) at strain rates of:					
	1.28e-5/sec	1.28e-4/sec	2.56e-4/sec	1.28e-3/sec	2.56e-3/sec	1.28e-2/sec
BiSn Q	30	42	53	69	74	86
BiSn SC	43	52	54	69	67	80
SnBi Q	---	47	70	85	100	125
SnBi SC	---	85	83	98	98	98
BiSnSb Q	34	62	65	66	83	84
BiSnSb SC	---	72	73	68	77	72

TABLE IX FLOW STRESS AT 10% STRAIN

SAMPLE	10% Flow Stress (MPa) at strain rates of:					
	1.28e-5/sec	1.28e-4/sec	2.56e-4/sec	1.28e-3/sec	2.56e-3/sec	1.28e-2/sec
BiSn Q	28	52	56	78	86	106
BiSn SC	44	67	70	86	88	100
SnBi Q	--	54	72	97	109	140
SnBi SC	--	95	103	123	124	135
BiSnSb Q	47	86	85	98	113	123
BiSnSb SC	--	95	98	100	109	112

TABLE X FLOW STRESS AT 20% STRAIN

SAMPLE	20% Flow Stress (MPa) at strain rates of:					
	1.28e-5/sec	1.28e-4/sec	2.56e-4/sec	1.28e-3/sec	2.56e-3/sec	1.28e-2/sec
BiSn Q	25	50	53	78	88	119
BiSn SC	42	71	79	100	106	125
SnBi Q	--	58	56	88	104	148
SnBi SC	--	91	105	136	143	171
BiSnSb Q	40	89	88	117	133	156
BiSnSb SC	--	100	110	130	135	144

From the stress-strain data log-log plots were constructed and a range for the value of the strain rate sensitivity factor determined for each composition and cooling rate. Figures 27 (tin rich), 28 (bismuth rich), and 29 (bismuth rich alloyed with antimony) show the plots for each of the two cooling rates. From these it can be seen that the quenched samples had a higher strain rate sensitivity in all cases. In terms of composition, the addition of Sb to Bi-Sn appeared to make it less sensitive to strain rate, regardless of cooling method.

Figures 30-35 show backscattered SEM micrographs of the tin rich binary, bismuth rich binary, and bismuth rich ternary alloys, respectively, both before and after the compression tests. Comparison of the microstructure before and after deformation shows that, in general, there was some coarsening of the microstructures during testing, possibly due to the relatively high homologous temperatures that induced dynamic recrystallizaton during deformation. Shear bands were also noted in the bismuth rich binary (Figure 32) and ternary (Figure 34) alloys for the slow cooled samples. Also, in the bismuth rich ternary alloy (Figure 35) a tin rich globular morphology was noted at the grain boundaries of the bismuth in the quenched sample.

In summary, from the data in tables VII, IX, and X it can be seen that the mechanical behavior of these alloys is heavily dependent on the cooling rate during processing. Furthermore, as room temperature is a high homologous temperature for bismuth-tin solder alloys and no true initial straight line portion of the stress-strain plots existed, Young's modulus values were not determined. The quenched samples exhibited a higher strain rate sensitivity than did the slow cooled samples. The bismuth rich composition alloyed with antimony, showed the lowest sensitivity to changes in strain rate.

V. CONCLUSIONS AND RECOMMENDATIONS

A. INTERMETALLIC GROWTH

This study examined the formation and growth of copper-tin and copper-antimony intermetallics at the interface between molten bismuth-tin solders and a copper substrate. The objective was to gain greater insight into the mechanisms involved in intermetallic growth as a functon of the length of time that the copper was in contact with the liquid solder, and the temperature of the solder bath.

In general the thickness increased with time as expected, with the notable exceptions of the two ternary alloys which saw a slight decrease in thickness at longer immersion times in a 400°C solder bath. The mechanism controlling growth appeared to be diffusion only in the case of the tin rich samples. In all other compositions growth seemed to be controlled by reactions taking place at the copper/intermetallic and/or intermetallic/liquid solder interfaces. Ternary addition of antimony resulted in a generally thicker intermetallic layer, except at longer immersion times, at 400°C as noted. This may be attributed to the formation of the CuSb intermetallics or the dissolution of the intermetallics.

B. COMPRESSION TESTING

Results of the compression tests showed that the strain rate sensitivity was highest in the tin rich samples, and lowest in the bismuth rich samples alloyed with antimony. Quenching appeared to result in a higher strain rate dependence. It was also noted that the samples may have been undergoing some recrystallization during testing.

C. FUTURE WORK

Fundamental research in the development of lead-free solders has only recently taken on a new importance as the need to eliminate lead-containing materials from the environment has become a national priority. The bismuth-tin system has shown promise as a replacement for lead-tin solders in certain applications, however further research is needed to understand and control its properties.

In the area of intermetallic growth, the efect of longer immersion times should be examined to see whether growth reaches some limiting value as suggested in previous studies, particularly in the ternary compositions where the kinetic constant appeared to become negative at high temperatures and longer immersion times. Additional research is also needed to determine the growth kinetics of the individual phases of the intermetallics that form, and their effect on the strength of the bond between the copper substrate and bismuth-tin solder. In terms of other mechanical properties, further study is needed to evaluate the thermal fatigue and creep resistance of the bulk solder, particularly in light of the low melting point of bismuth-tin solders. In addition the solderability of these compostions needs to be evaluated to see if there is any improvement over the eutectic composition.

It is hoped that this study can provice a basis on which to build in future work in the area of lead-free solders.

APPENDIX

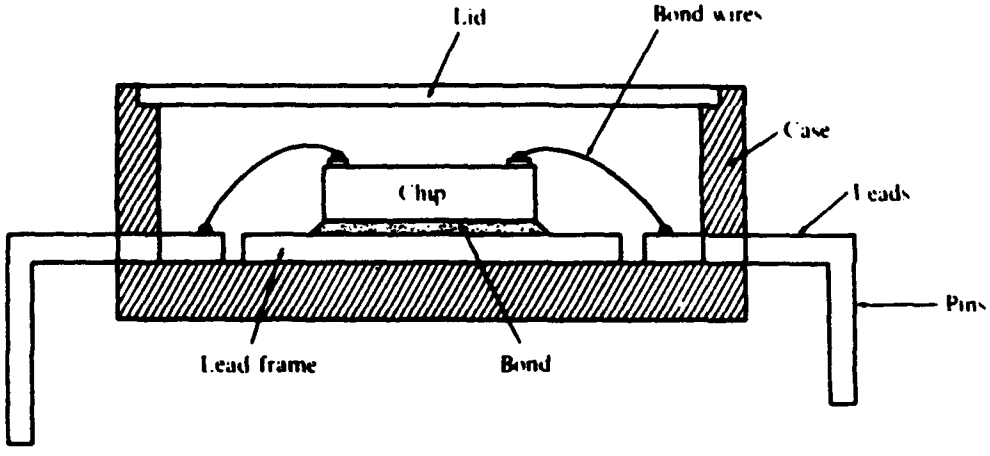

Figure 1 Typical features of a chip carrier [Ref. 2:p. 96].

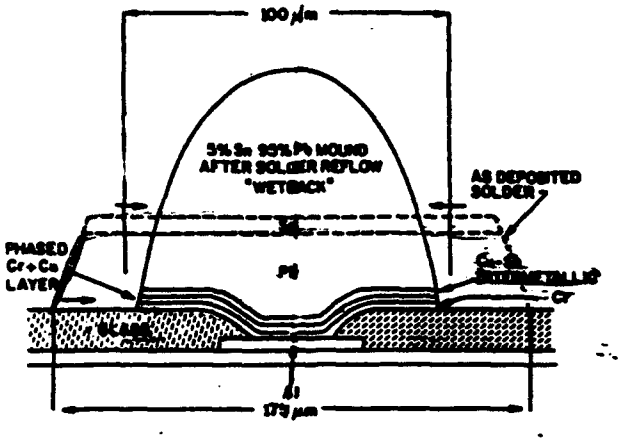

Figure 2 Cross section through solder ball as deposited and after reflowing.

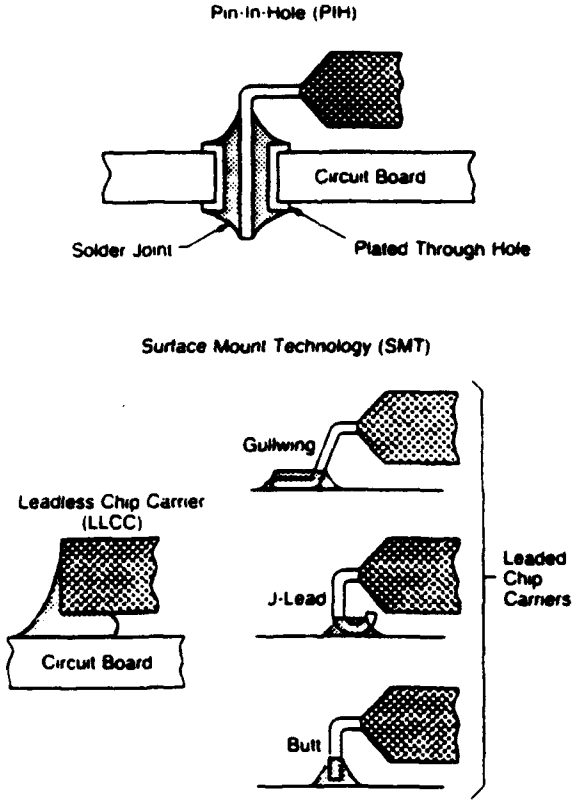

Figure 3 PIH and SMT Solder Joints [Ref. 4:p. 147].

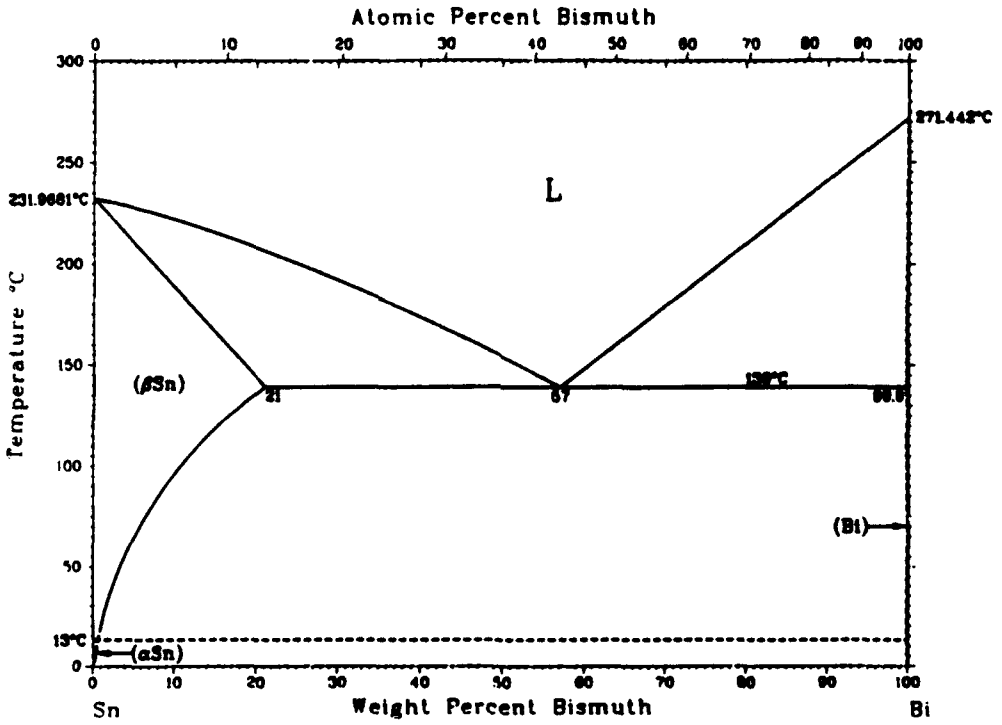

Figure 4 Binary phase diagram for bismuth-tin system.

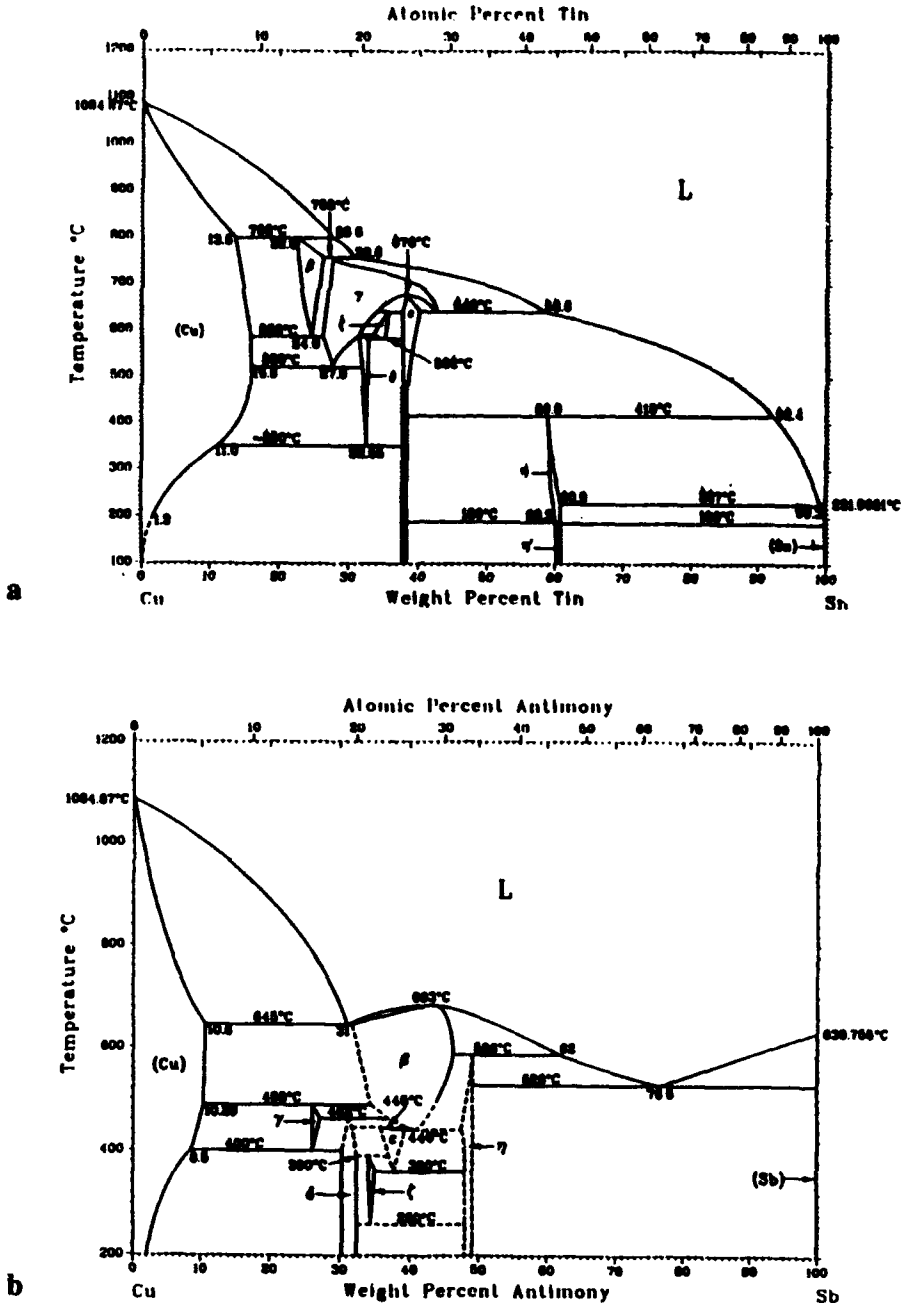

Figure 5 Binary phase diagrams for (a) Cu-Sn and (b) Cu-Sb.

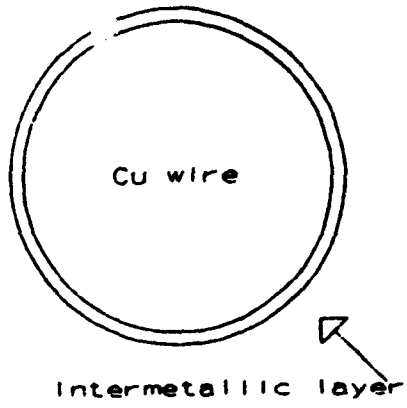

Figure 6 Location of intermetallic viewed on copper wires.

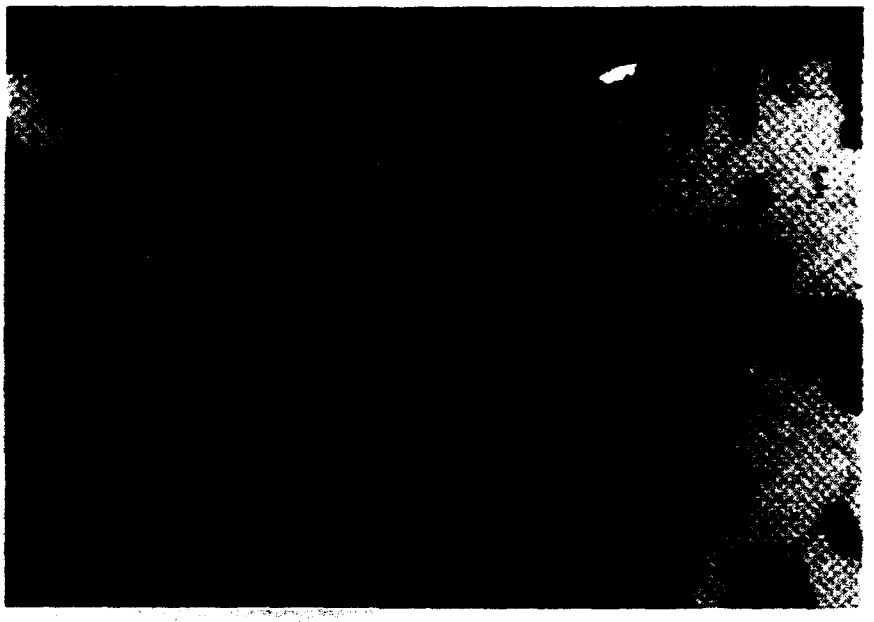

a

b

Figure 7 Backscattered electron micrographs of the intermetallic layer growth on copper wire immersed in 30Bi-70Sn liquid solder at 300°C. (a) 2 minutes, (b) 5 minutes. Darkest region is copper wire. Solder consists of bismuth (light grey), and tin (darker regions). Intermetallic forms as uneven layer at Cu/solder interface.

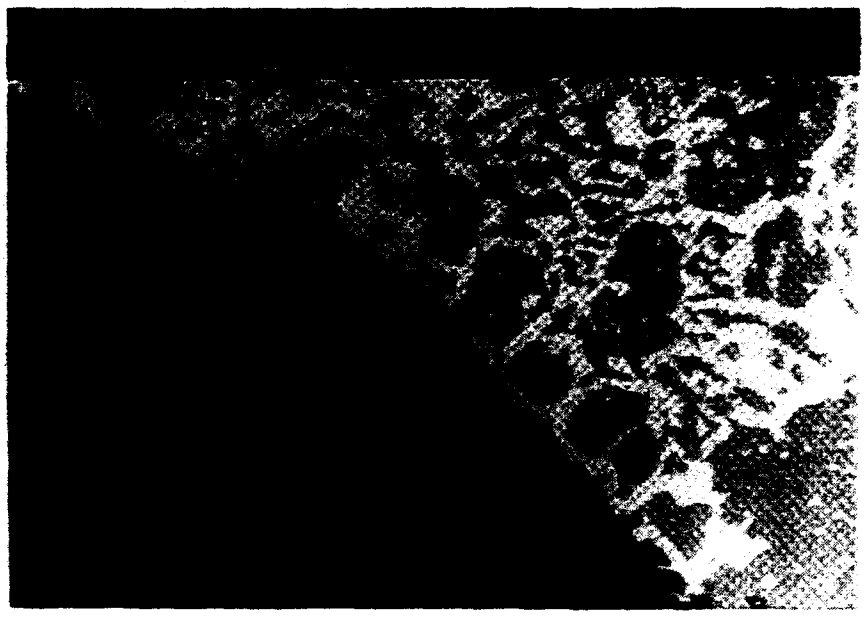

Figure 7 (cont'd) (c) 10 minute immersion at 300°C.

Figure 8 Cross section of intermetallic formed after a 5 minute immersion at 350°C, showing both phases: Cu_6Sn_5 (light region immediately below solder and Cu_3Sn (darker region between Cu and Cu_6Sn_5). Compositions were verified by EDXS analysis.

a

b

Figure 9 SEM micrographs of surface of Cu_6Sn_5 on copper wire immersed for 1/2min. (a) 250°C. (b) 300°C.

Figure 9 (cont'd) (c) 1/2 minute immersion at 350°C.

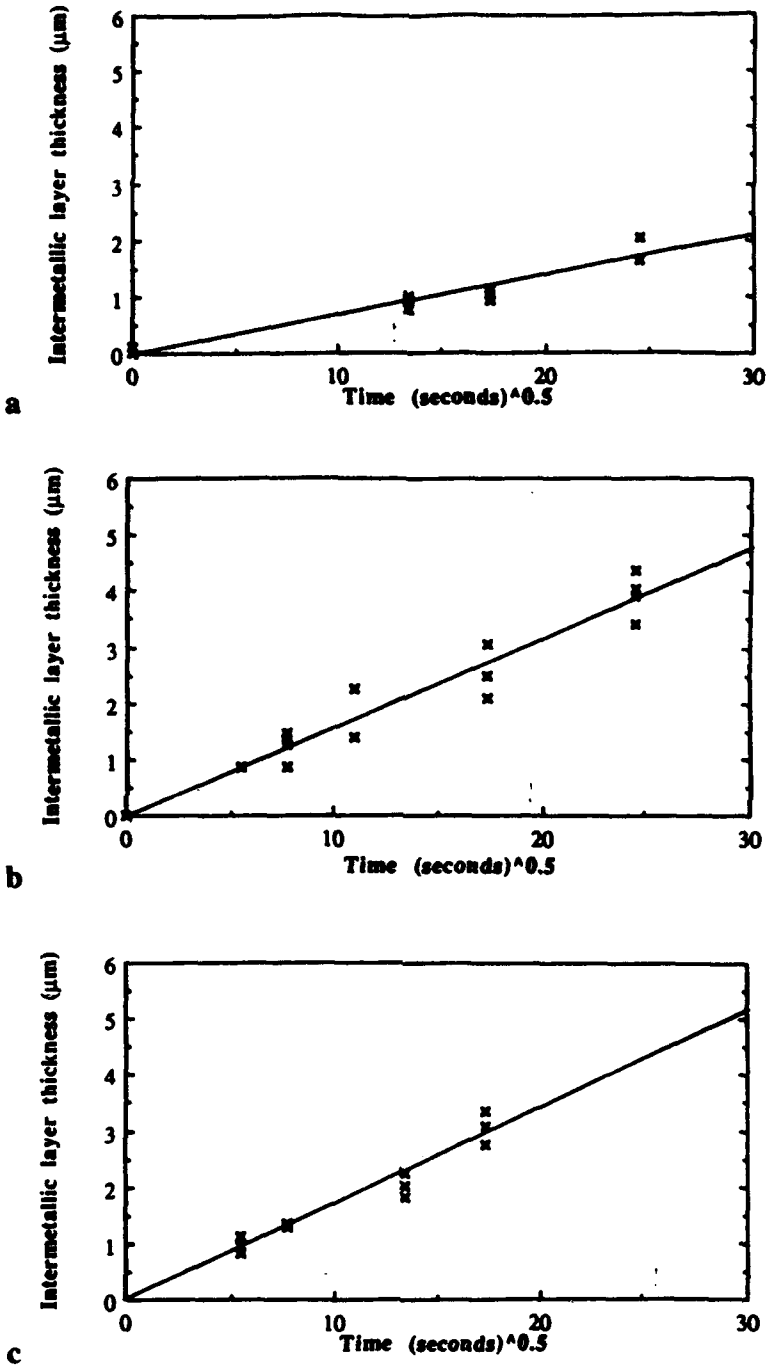

Figure 10 *Results of growth measurements in 70Sn-30Bi solder,* plotted as thickness versus time$^{1/2}$ for diffusion controlled growth. (a) 250°C. (b) 300°C. (c) 350°C.

a

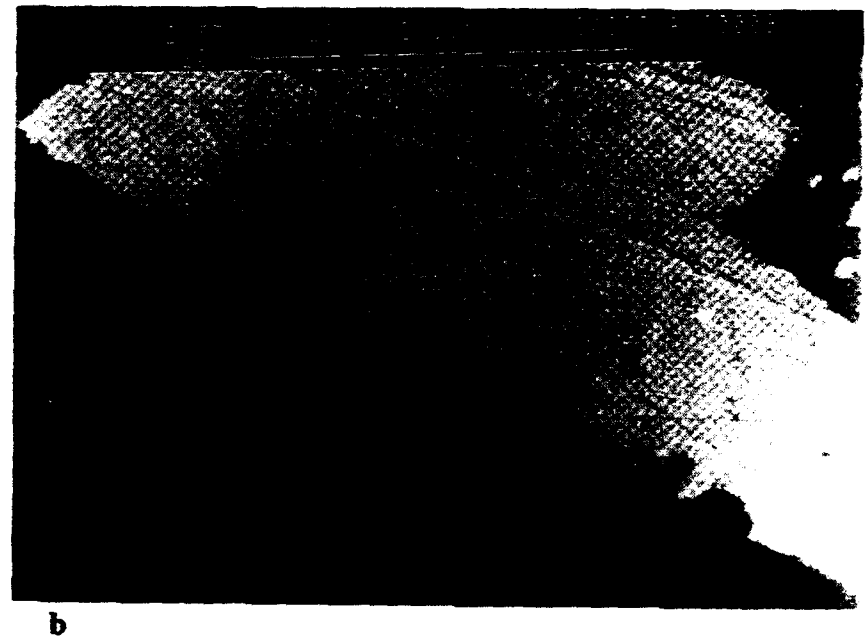

b

Figure 11 SEM micrographs of cross section of copper wire immersed in bismuth rich solder bath. (a) 250°C for 1/2 minute. (b) 350°C for 5 minutes.

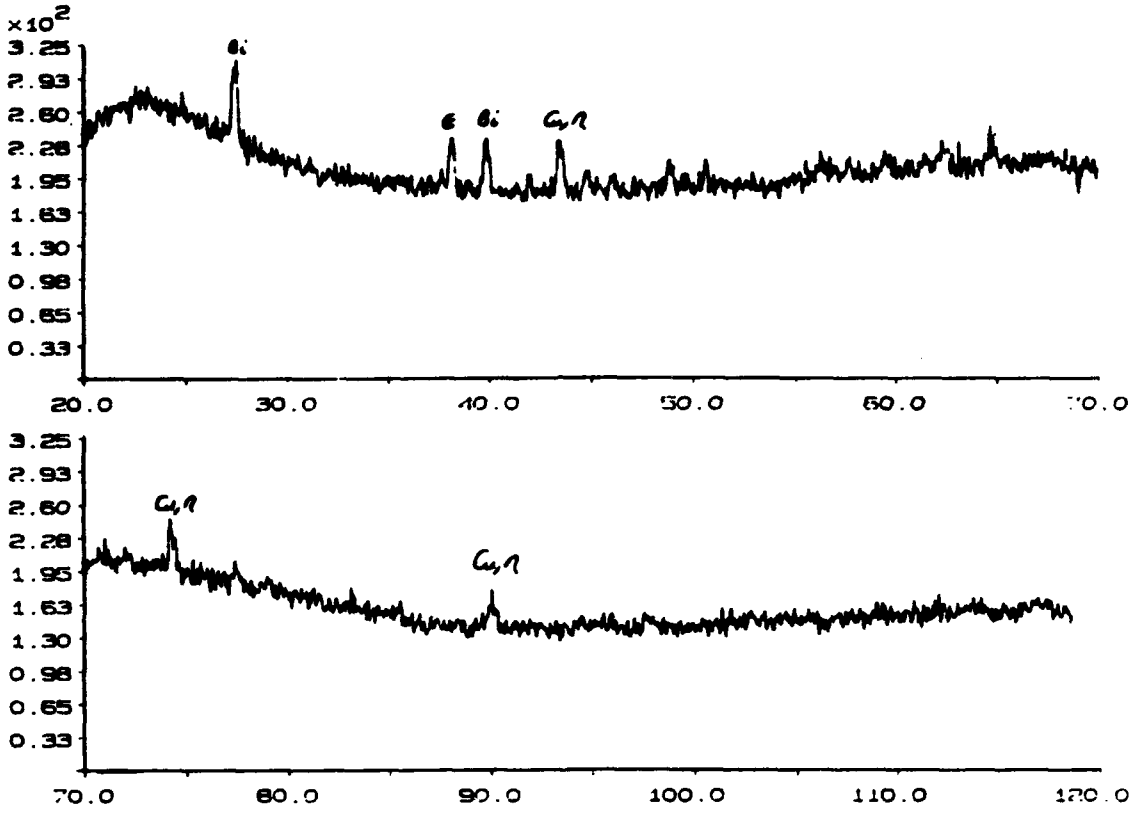

Figure 12 X-ray scan of surface of intermetallic layer on copper wire immersed in a solder bath (70Bi-30Sn) at 350°C for 5 minutes.

ε = Cu_3Sn and η = Cu_6Sn_5.

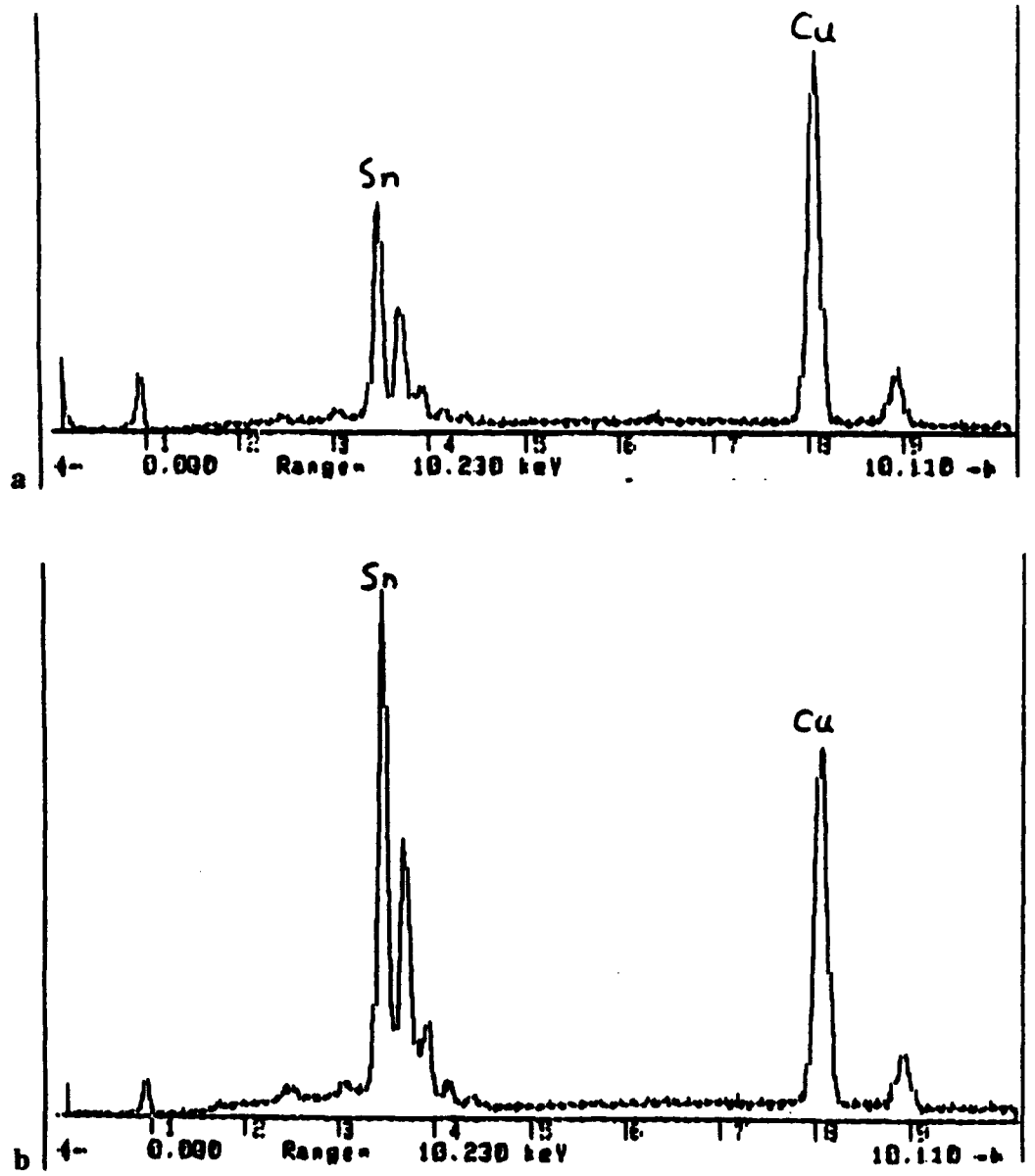

Figure 13 Results of EDX microprobe analysis. (a) Cu rich (Cu_3Sn) in the region near the Cu substrate. (b) Cu_6Sn_5 in the region near the solder.

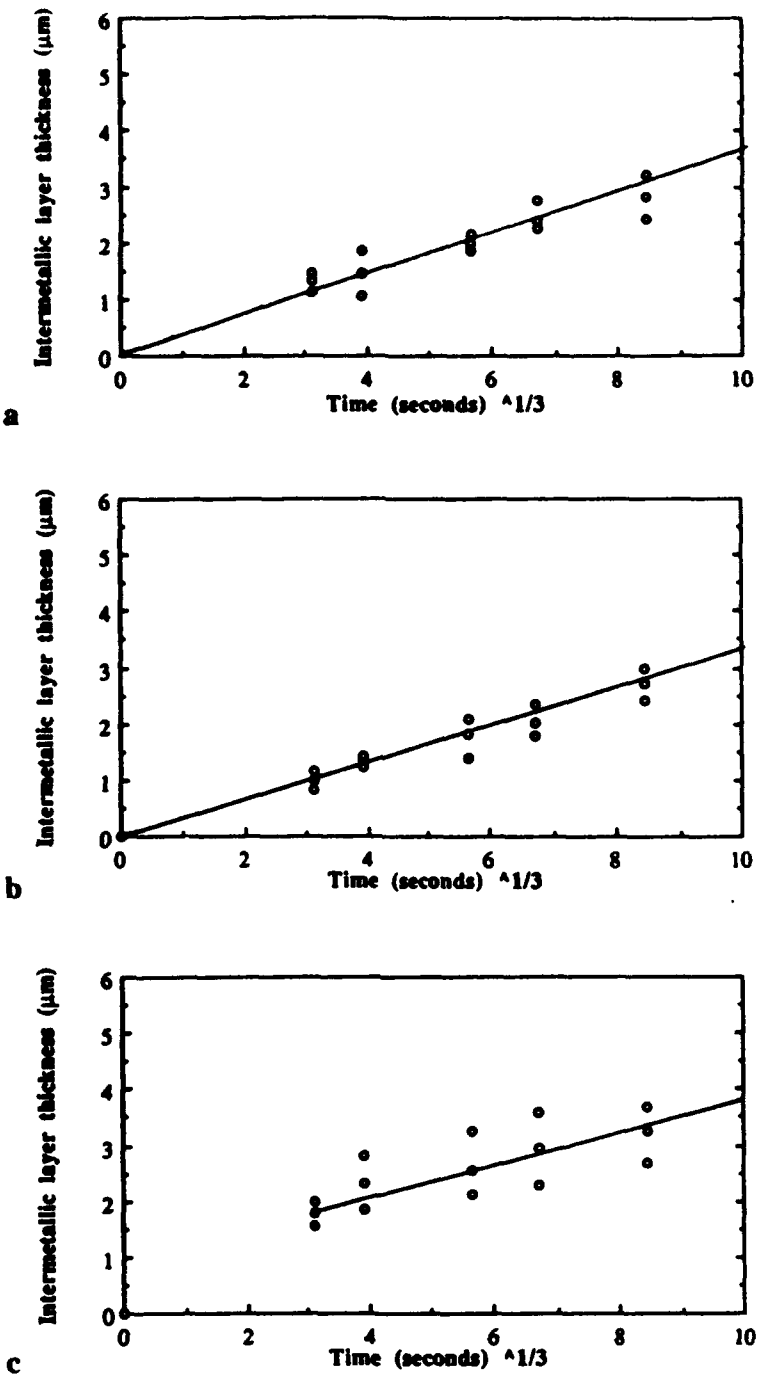

Figure 14 Results of growth measurements in 70Bi-30Sn solder plotted as thickness versus time$^{1/3}$ for interface controlled growth. (a) 250°C. (b) 300°C. (c) 350°C.

a

b

Figure 15 Surface morphology of intermetallic layer (Cu_6Sn_5) on copper wire after immersion in bismuth rich solder. (a) 250°C for 1 minute. (b) 350°C for 10 minutes.

a

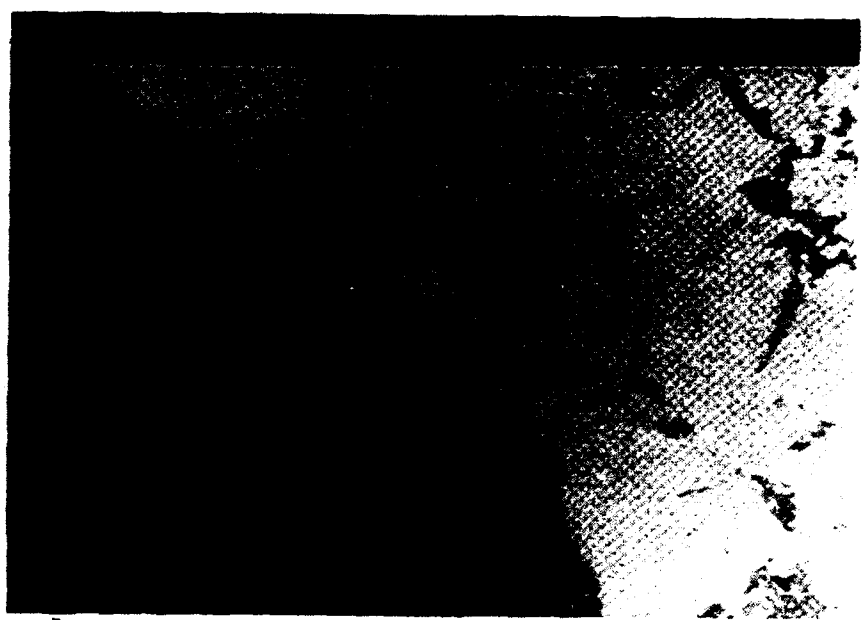

b

Figure 16 Cross section of copper wire immersed in 68Bi-29Sn-3Sb solder bath at 350°C. (a) 1 minute. (b) 10 minutes

a

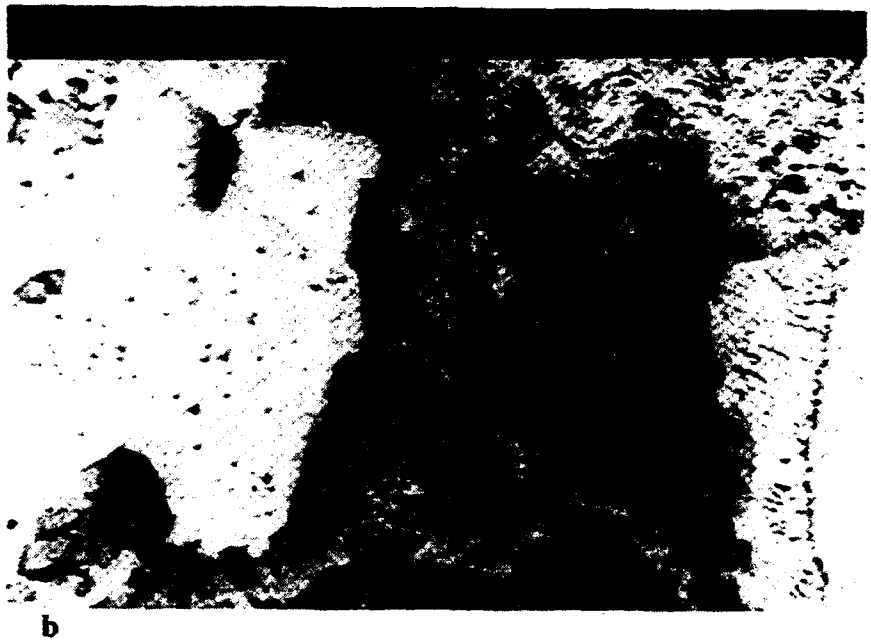

b

Figure 17 SEM micrographs showing surface morphology of intermetallics found on copper wire immersed at 300°C for 5min. (a) $Cu_{3.3}Sb$. (b) Cu_6Sn_5.

Figure 18 SEM micrograph of surface morphology of the intermetallic formed by immersing in 68Bi-29Sn-3Sb liquid solder at 400°C for 10 minutes.

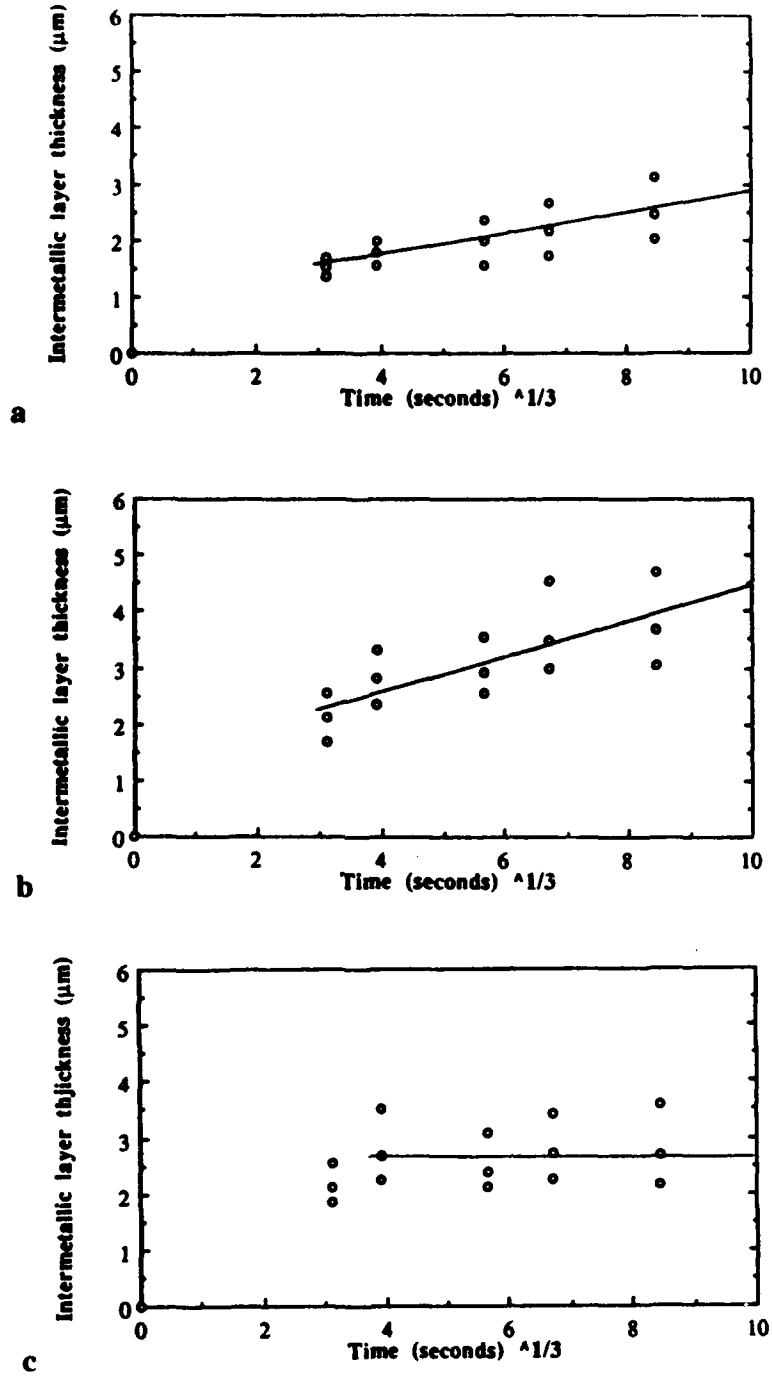

Figure 19 Results of growth measurements in 68Bi-29Sn-3Sb solder, plotted as thickness versus time$^{1/3}$ for interface controlled growth. (a) 300°C. (b) 350°C. (c) 400°C.

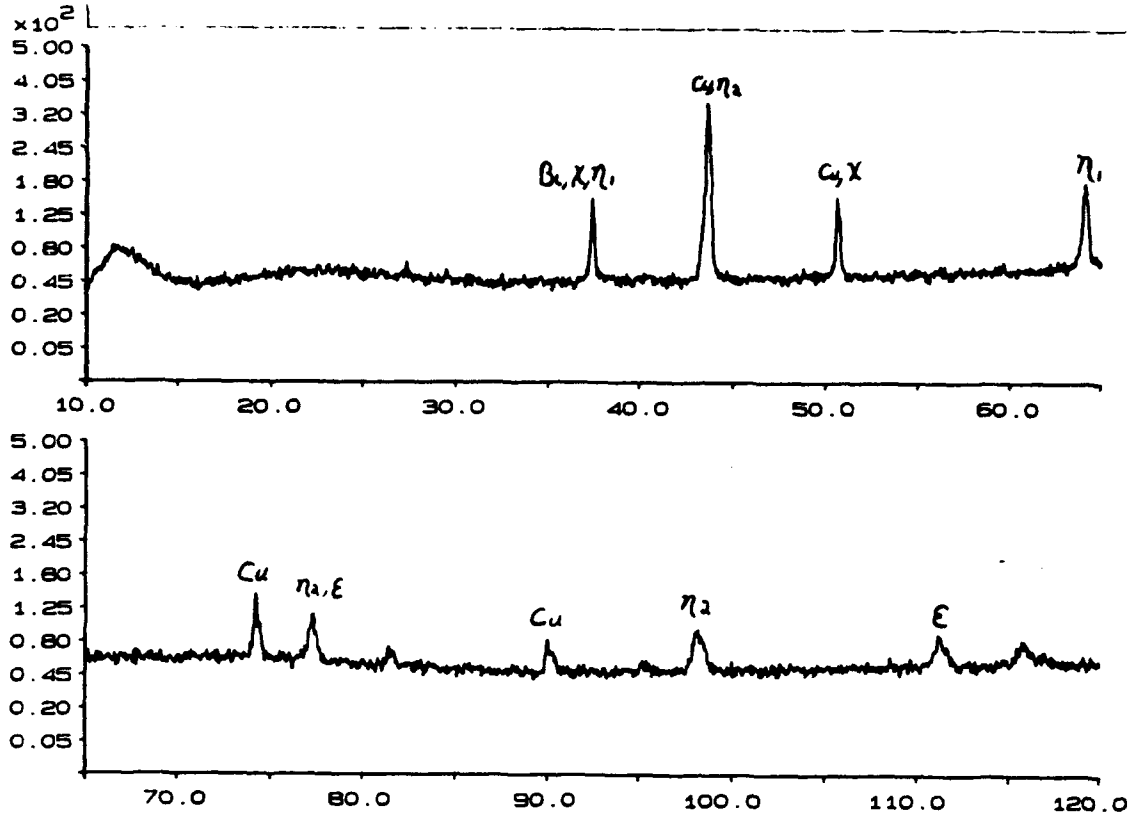

Figure 20 X-ray scan of intermetallics formed on the surface of copper wire immersed in 68Bi-29Sn-3SB solder at 350°C for 3 minutes.

η_1 = $Cu_{3.3}Sb$; η_2 = Cu_6Sn_5; χ = Cu_3Sb; ε = Cu_3Sn.

Figure 21 SEM micrographs of cross sections of the intermetallic layer on Cu (dark) after immersion in 37Bi-58Sn-5Cu liquid solder. (a) 300°C for 10 minutes. (b) 350°C for 10 minutes. Note presence of voids at Cu/intermetallic interface.

Figure 21 (cont'd) (c) 400° C for 1/2 minute. Note absence of voids at short immersion time.

a

b

Figure 22 SEM micrographs of cross section of intermetallic layer on copper wire immersed in 350°C 37Bi-58Sn-5Cu solder bath. (a) 3 minutes. (b) 5 minutes. Note presence of voids at longer time.

Figure 22 (cont'd) (c) 10 minutes. Note presence of voids at long immersion time.

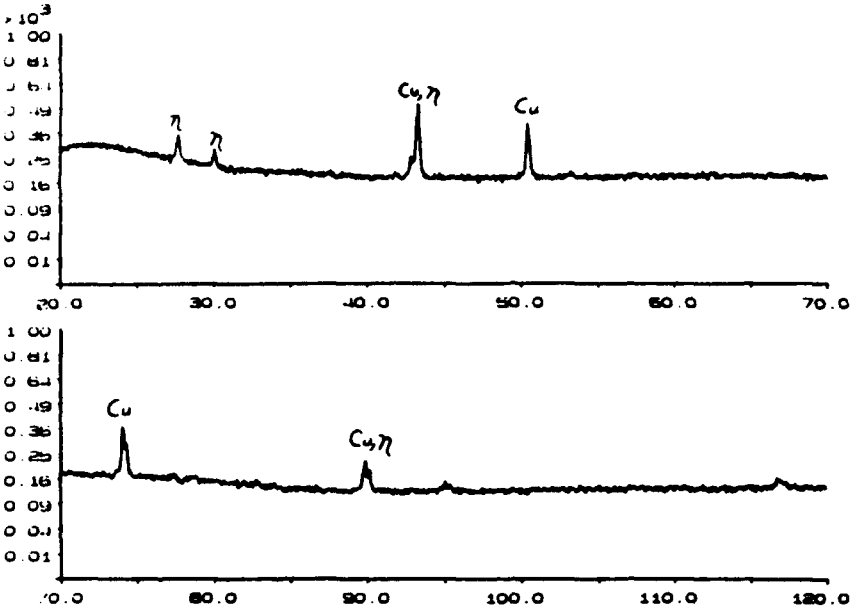

a

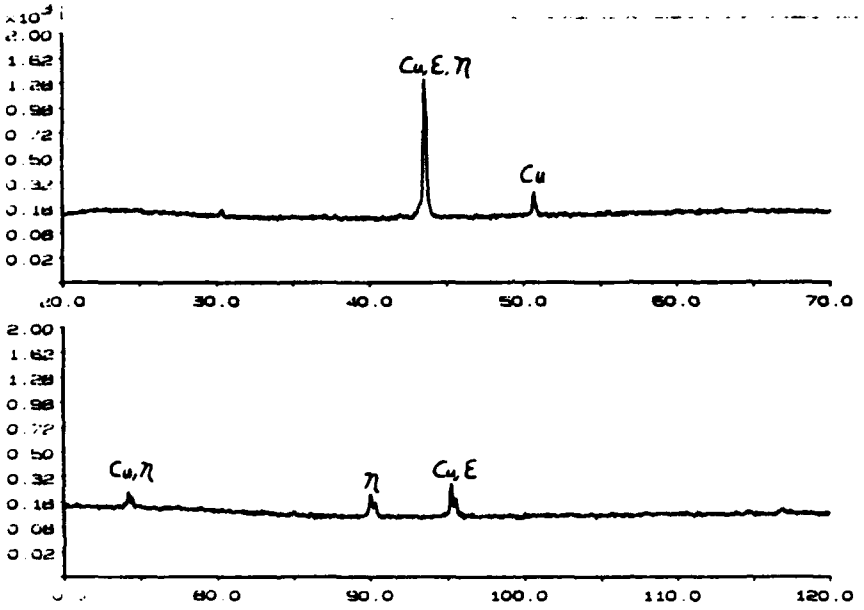

b

Figure 23 X-ray diffraction scans of surface of intermetallic layer. (a) 300°C. (b) 400°C. ε = Cu_3Sn; η = Cu_6Sn_5.

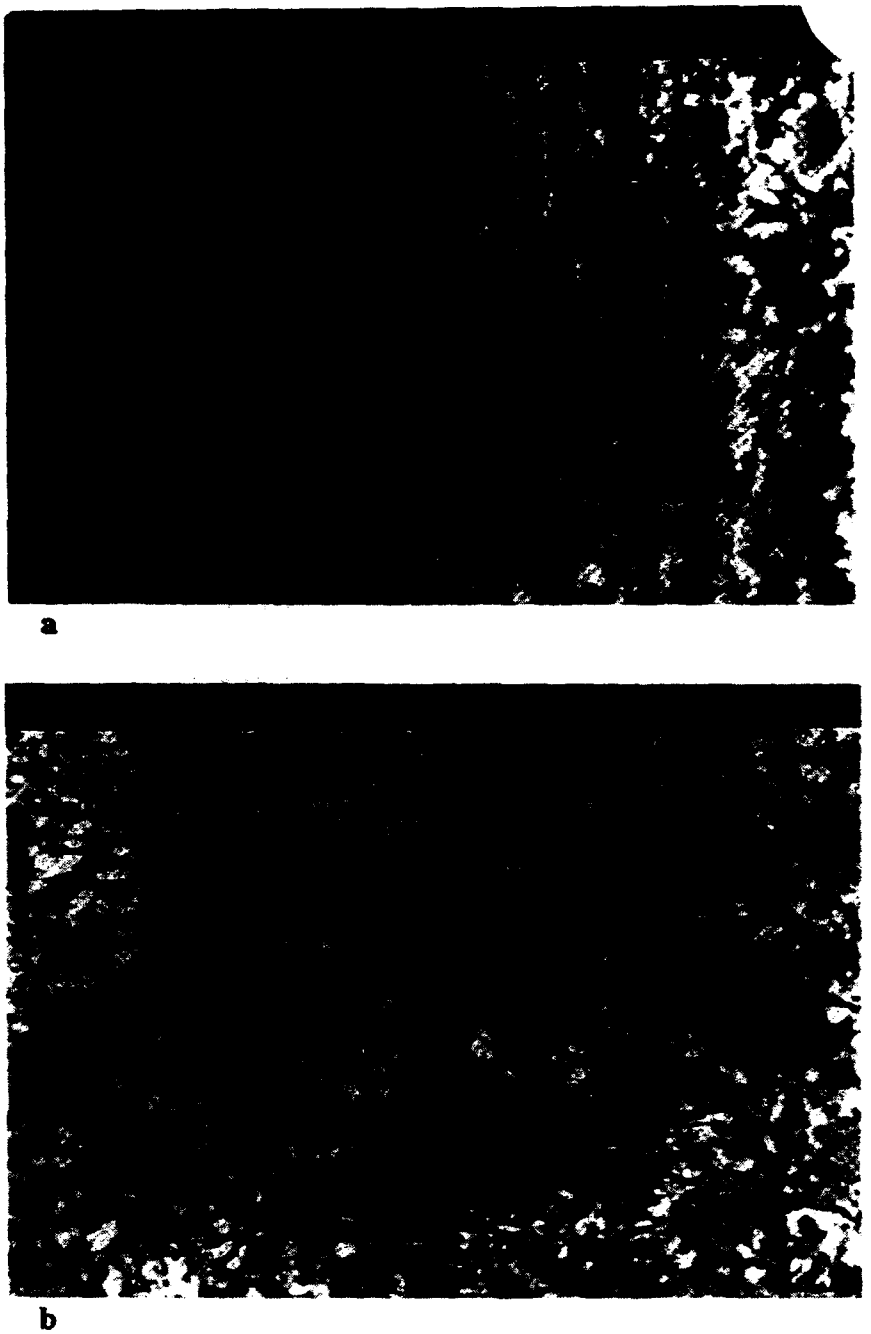

Figure 24 SEM micrographs of surface morphology of intermetallics formed on copper wire immersed in 37Bi-58Sn-5Cu solder bath. (a) 1/2 minute at 300°C. (b) 5 minutes at 350°C.

Figure 24 (cont'd) (c) 10 minutes at 400°C.

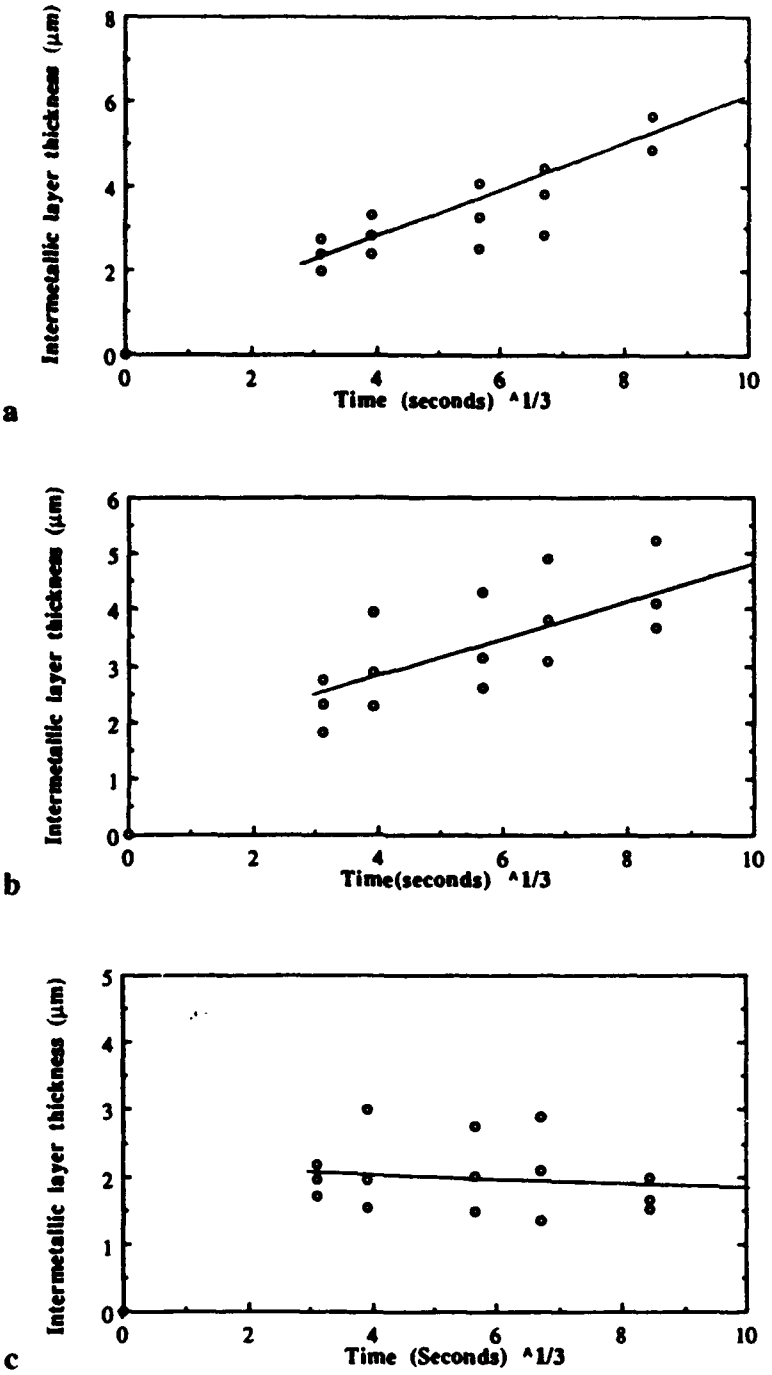

Figure 25 Results of growth measurements in 37Bi-58Sn-5Cu solder, plotted as thickness versus time$^{1/3}$ for interface controlled growth. (a) 300°C. (b) 350°C. (c) 400°C.

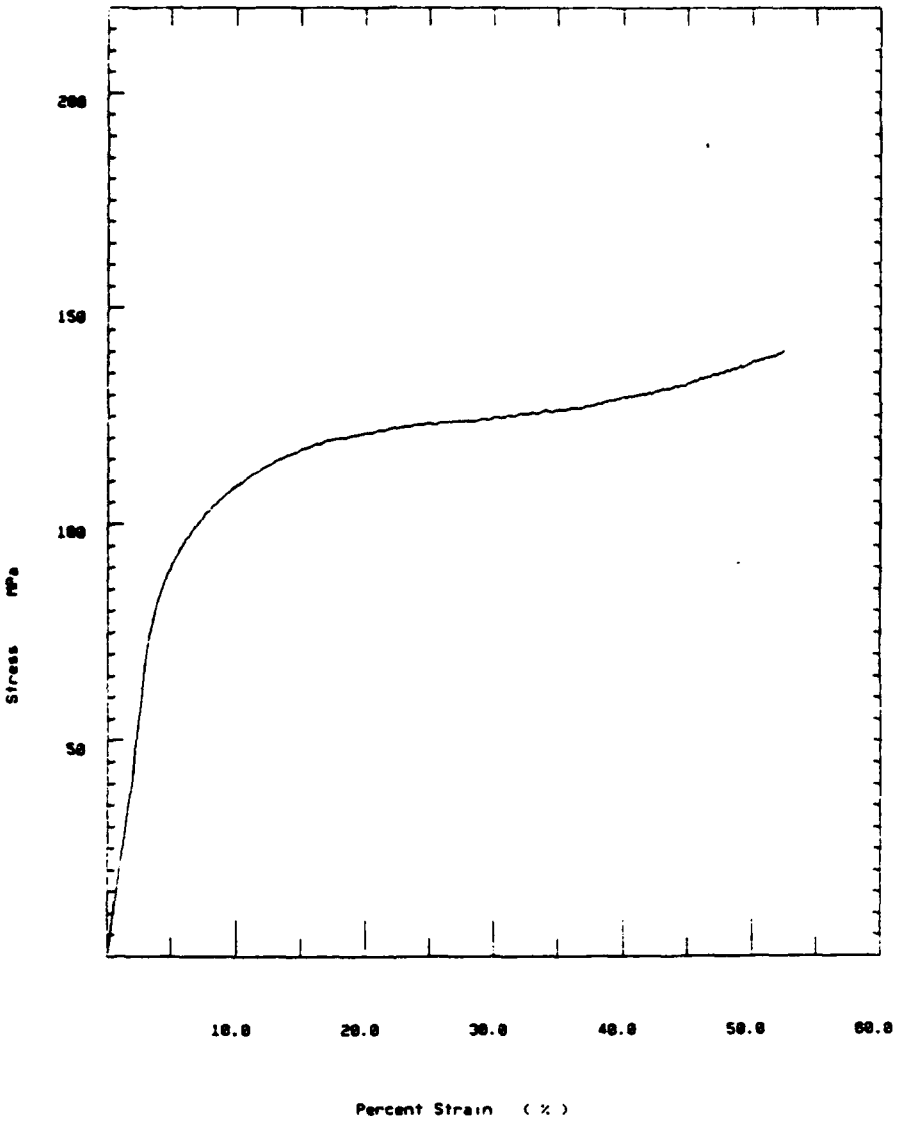

a

Figure 26 Stress vs % strain plots for compression tests of (70Bi-30Sn wt%) bulk solder tested at a strain rate of 0.0128/sec. (a) quenched.

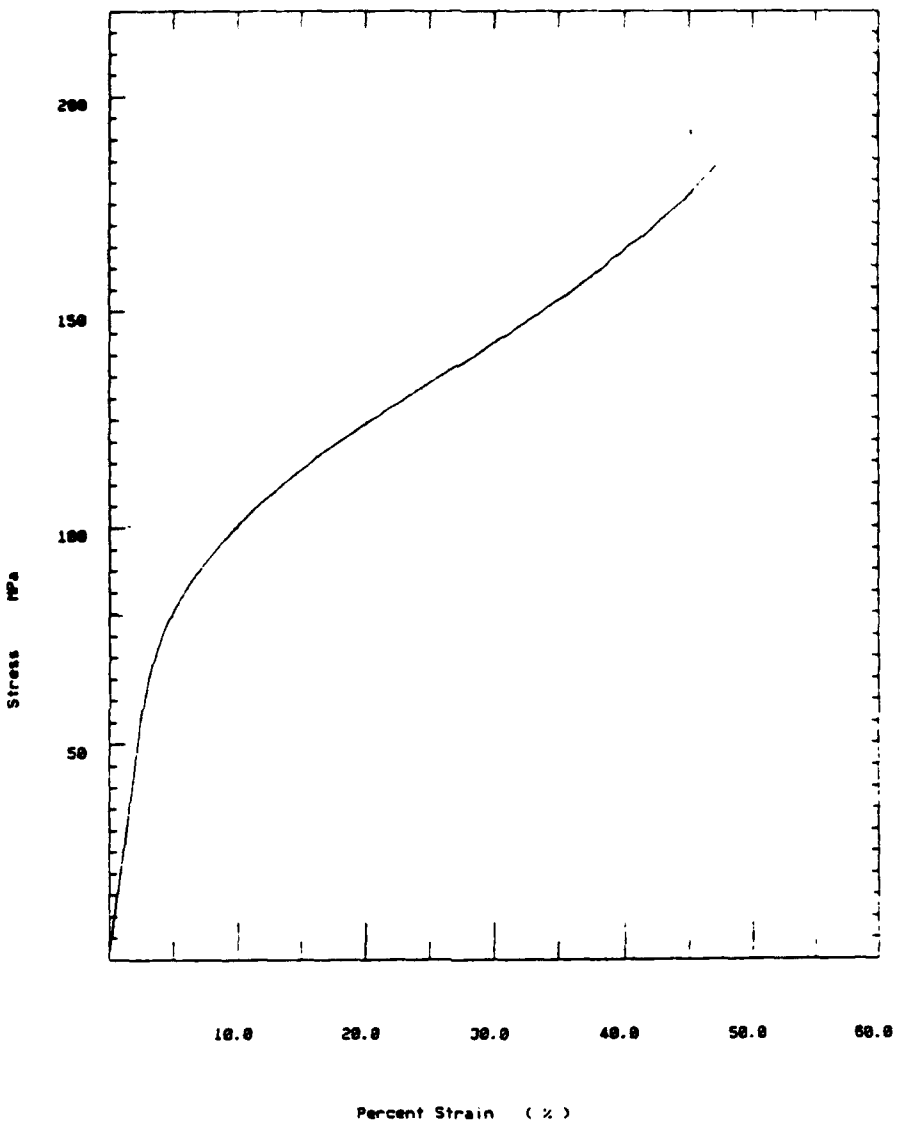

b

Figure 26 (cont'd) (b) slow-cooled.

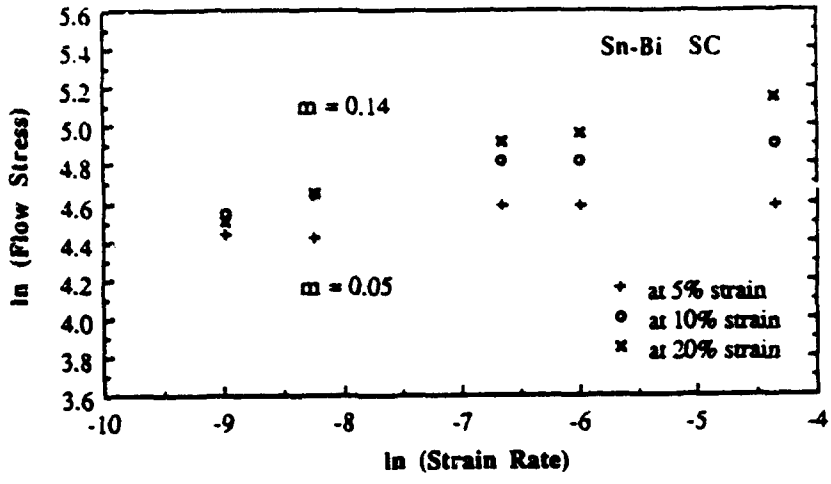

a

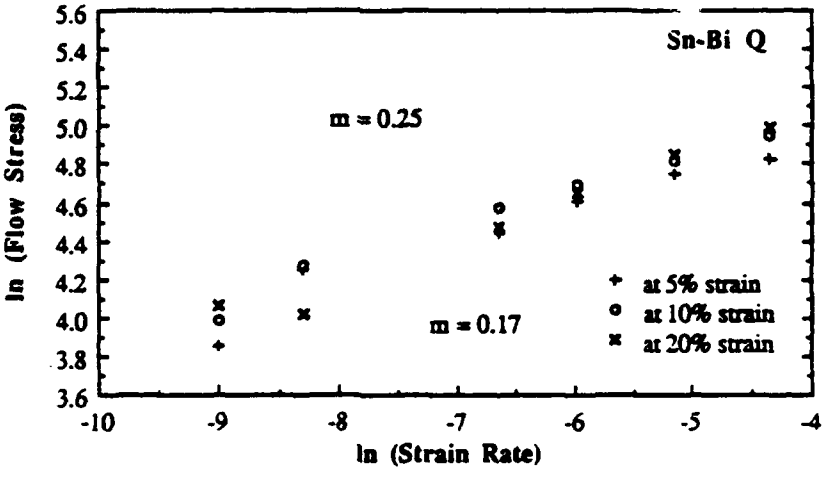

b

Figure 27 Log-log plots of flow stress vs strain rate for (70Sn-30Bi wt%) (a) slow cooled. (b) quenched.

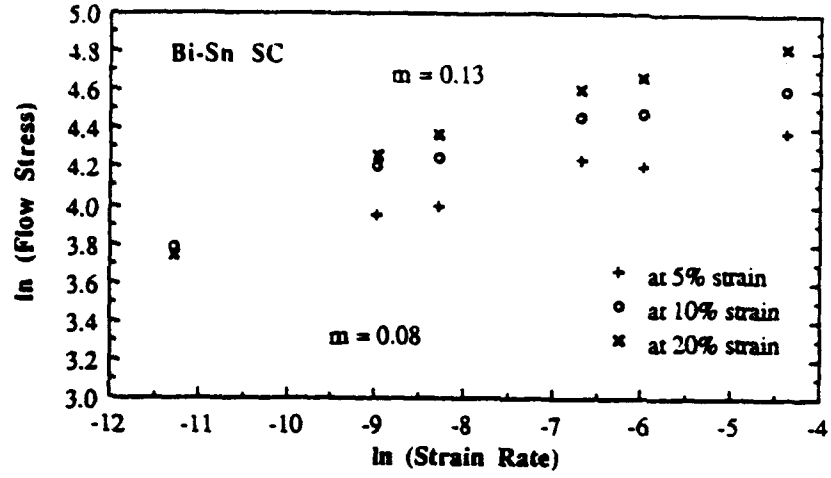

a

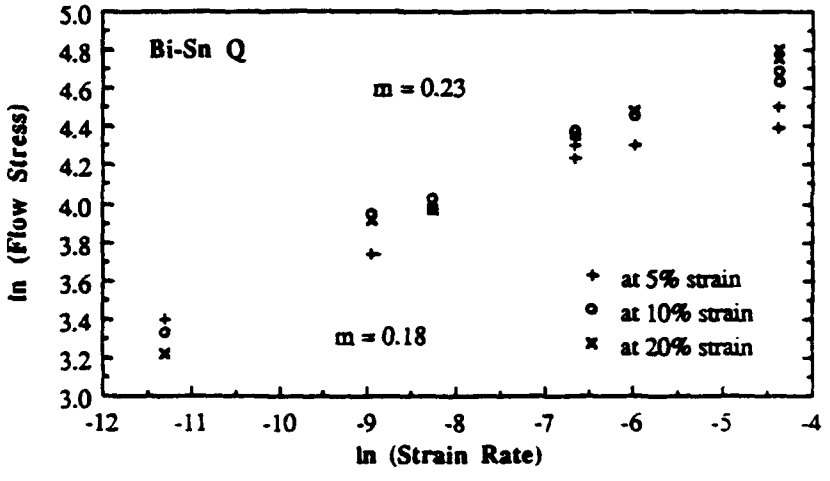

b

Figure 28 Log-log plots of flow stress vs strain rate for (70Bi-30Sn wt%) (a) slow cooled. (b) quenched.

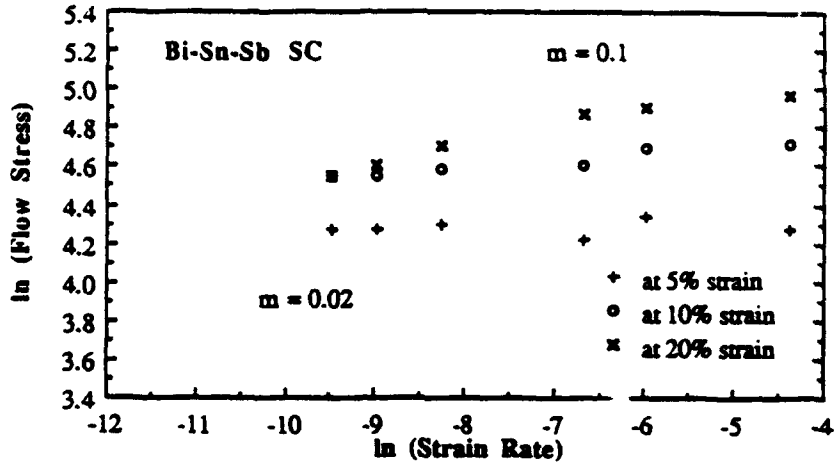

a

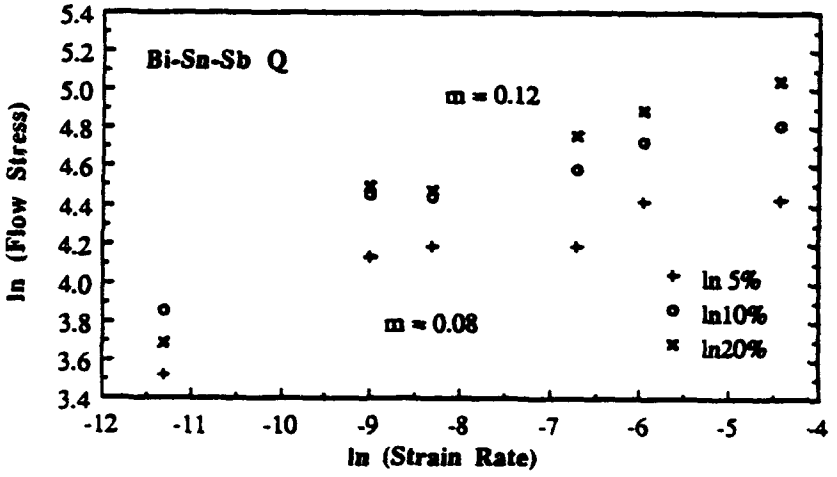

b

Figure 29 Log-log plots of flow stress vs strain rate for (68Bi-29Sn-3Sb wt%) (a) slow cooled. (b) quenched.

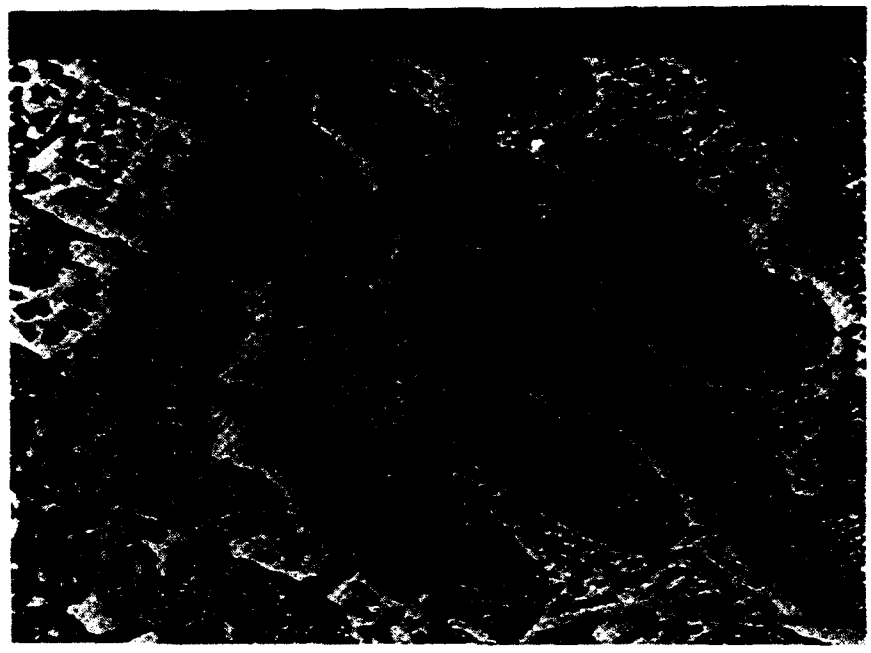

a

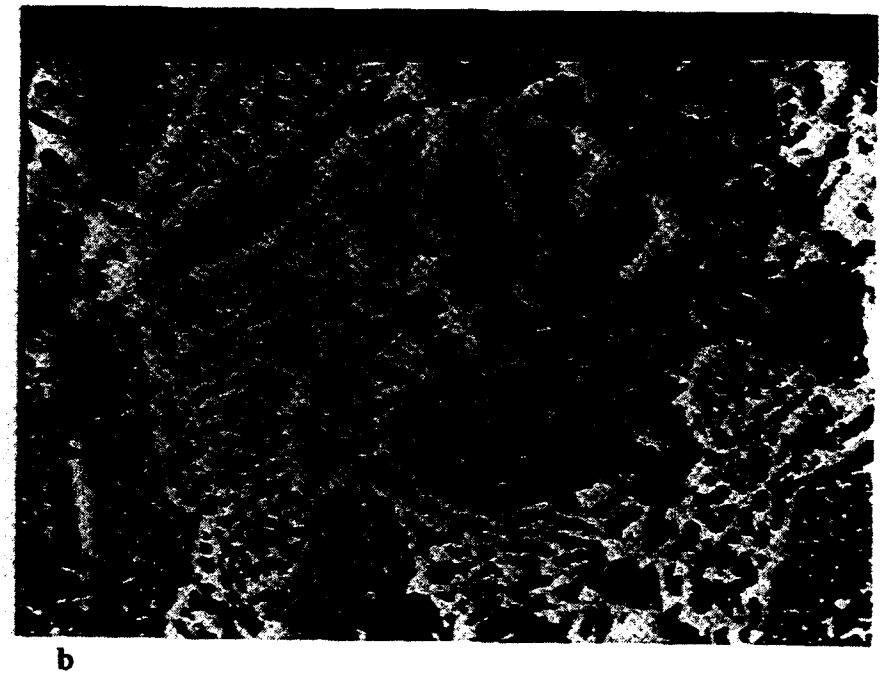

b

Figure 30 Microstructure of quenched (70Sn-30Bi wt%) Bulk solder (a) before and (b) after compression testing at strain rate of 0.000128/sec.

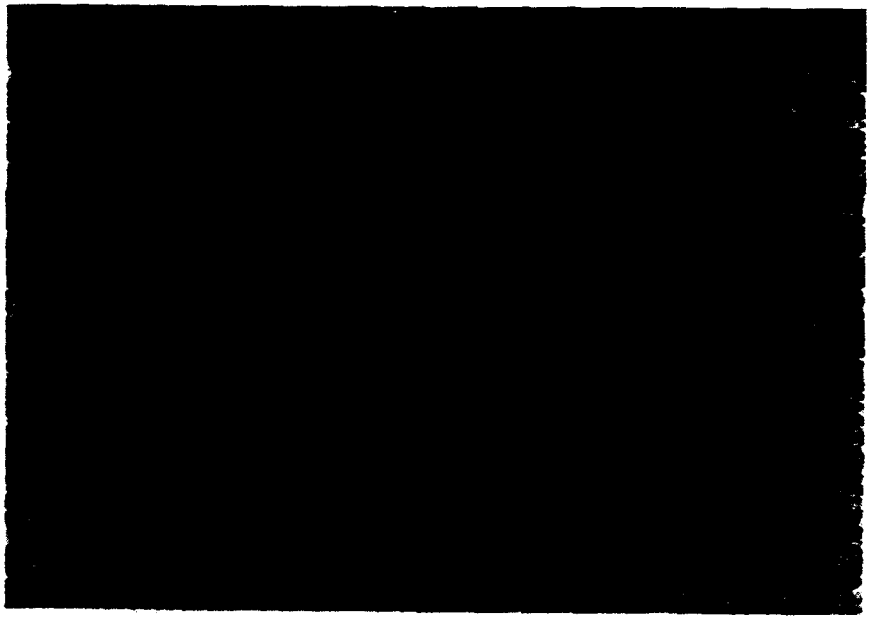

a

b

Figure 31 Microstructure of slow cooled (70Sn-30Bi wt%) bulk solder (a) before and (b) after compression testing at a strain rate of 0.000128/sec.

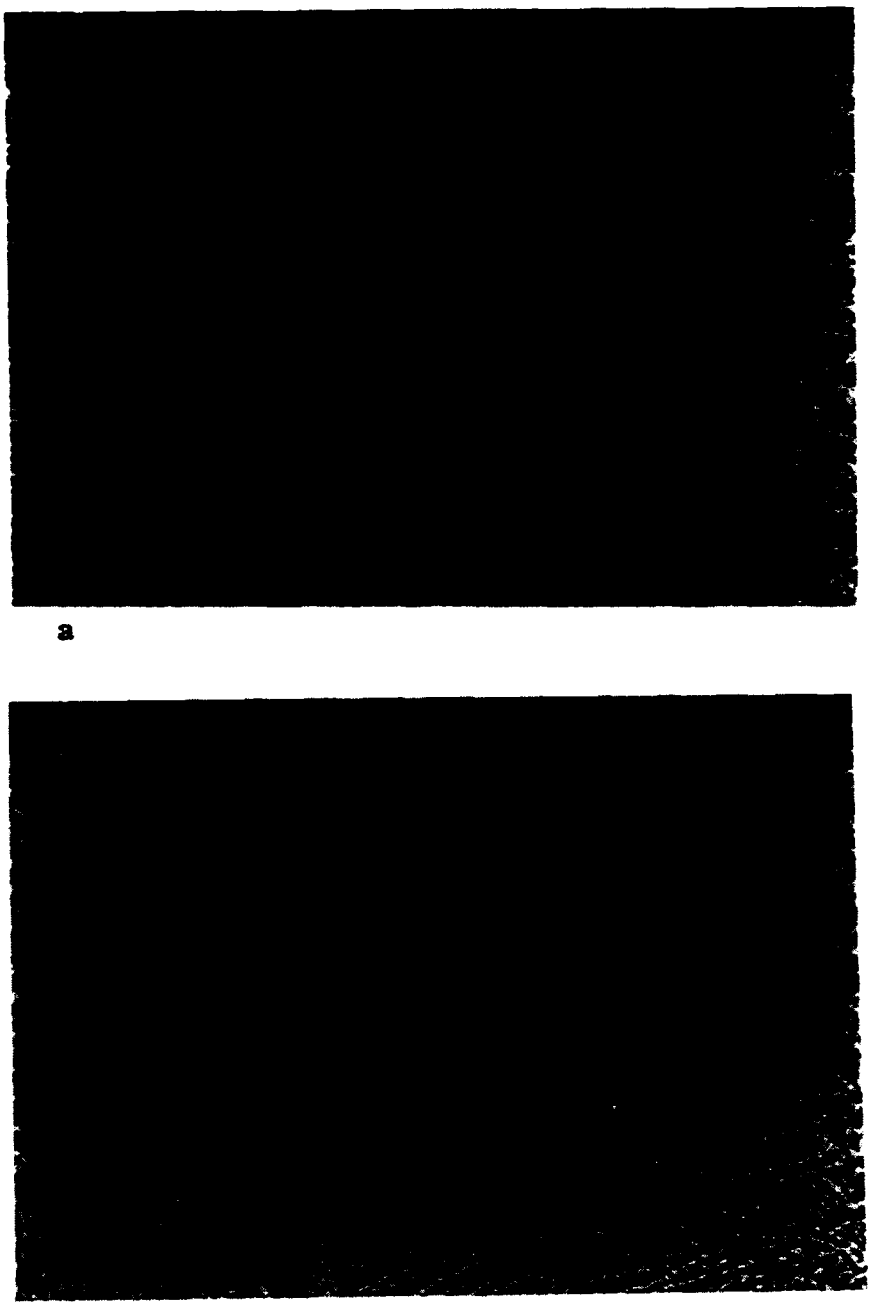

Figure 32 Microstructure of quenched (70Bi-30Sn wt%) bulk solder (a) before and (b) after compression testing at a strain rate of 0.000128/sec.

a

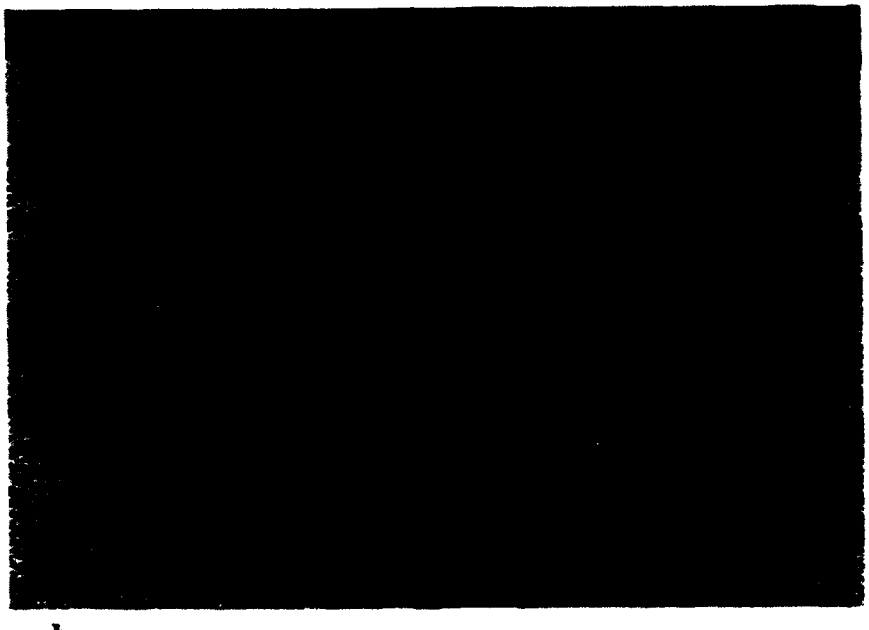

b

Figure 33 Microstructure of slow cooled (70Bi-30Sn wt%) bulk solder (a) before and (b) after compression testing at a strain rate of 0.000128/sec.

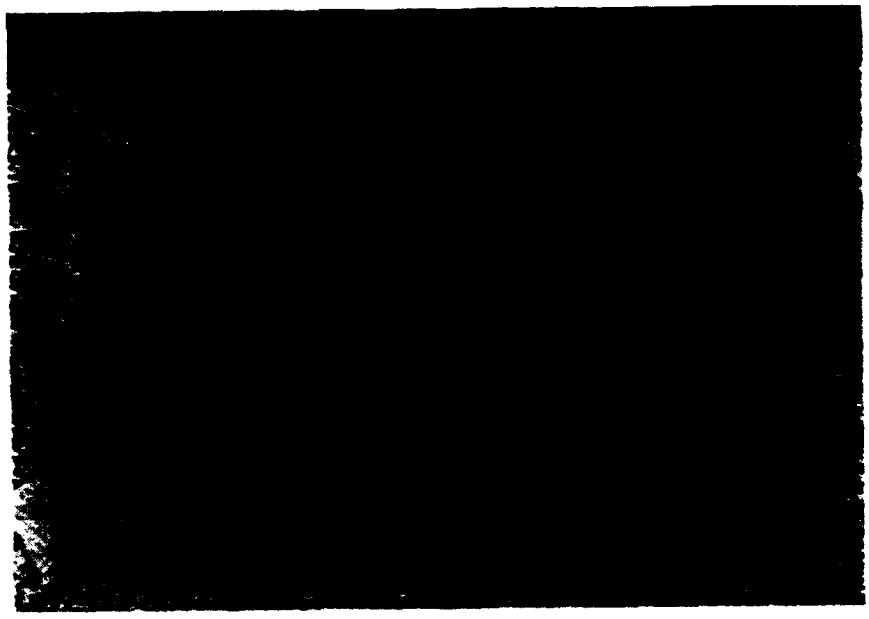

a

b

Figure 34 Microstructure of quenched (68Bi-29Sn-3Sb wt%) bulk solder (a) before and (b) after compression testing at a strain rate of 0.000128/sec.

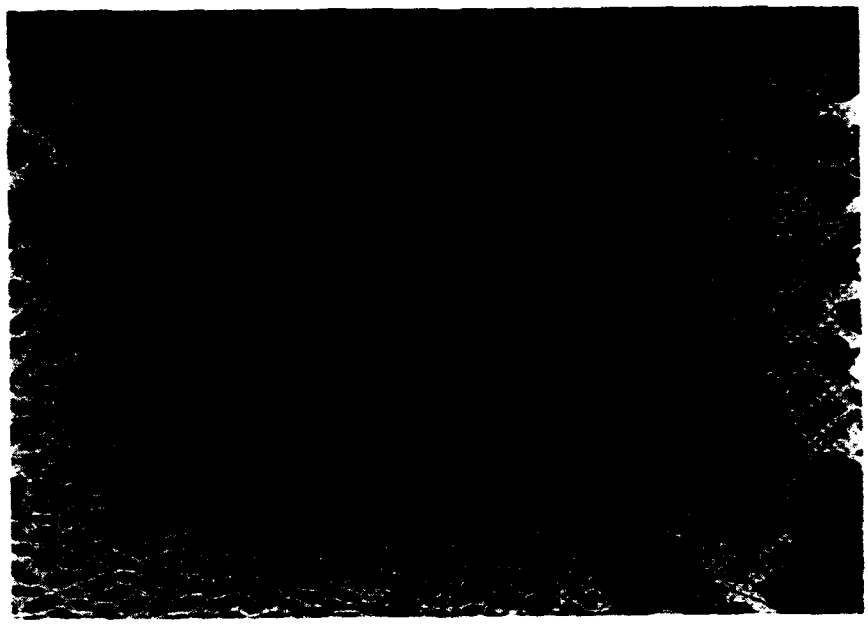

a

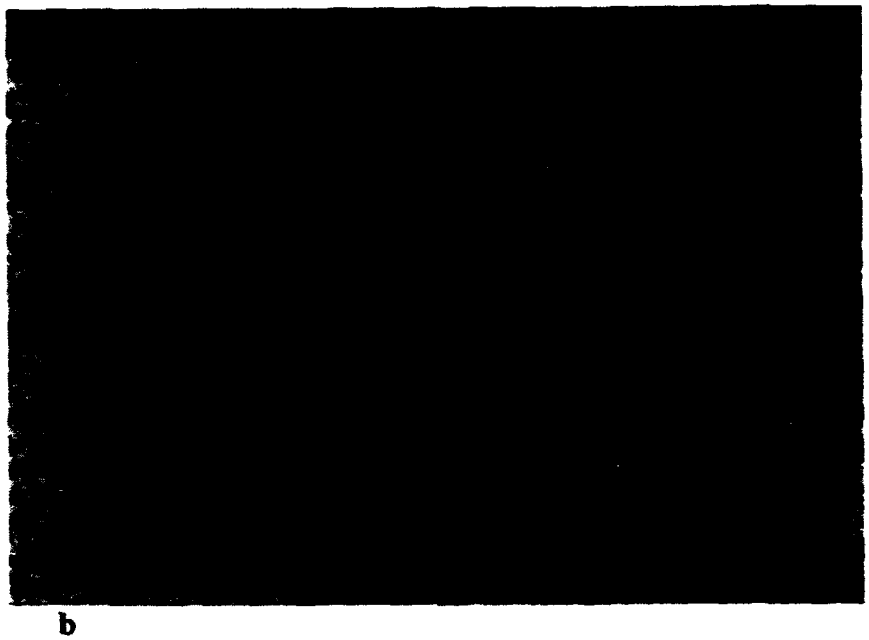

b

Figure 35 Microstructure of slow cooled (68Bi-29Sn-3Sb wt%) bulk solder (a) before and (b) after compression testing at a strain rate of 0.000128/sec.

LIST OF REFERENCES

1. Vianco, P.T., and Frear, D.R., "Issues in the Replacement of Lead Bearing Solders," *JOM The Journal of the Minerals, Metals, and Materials Society*, volume 45, number 7, July 1993.

2. Dally, J.W., *Packaging of Electronic Systems A Mechanical Engineering Approach*, McGraw Hill Publishing Company, 1990.

3. Pecht, M.G., *Soldering Processes and Equipment*, Wiley-Interscience Publications, 1993.

4. Fine, M.E., and Jeanotte, D.A., "Soft Solder - General Principles and Fatigue Lifetime Estimation," *Micro Electronic Packaging Technology Materials and Processes Conference Proceedings*, Edited by W.T. Shieh, ASM Publishing, 1989.

5. SunWoo, A.J., Morris, J.W., and Lucey, G.K., "The Growth of Cu-Sn Intermetallics at a Pretinned Copper-Solder Interface," *Metallurgical Transactions*, volume 23A, pp. 1323-1332, April 1992.

6. Morris, J.W., Tribula, D., Summers, T.S.E., and Grivas, D., "The Role of Microstructure in Thermal Fatigue of Pb-Sn Solder Joints,"*Solder Joint Reliability*, edited by John H.Lau, Von Nostrand Reinhold Publishing, 1991.

7. Browning, E., *Toxicity of Industrial Metals*, 2d ed., Butterworth and Company LTD. Publishing, 1969.

8. United States Congress, *Toxic Lead Reduction Act (S. 2637)*, Senators H. Reid, J. Lieberman, and W. Bradley, 1990.

9. United States Congress, *Lead Based Paint Hazard Abatement Act (H. 2922)*, Representatives B. Cardin, and H. Waxman, 1991.

10. United States Congress, *Lead Pollution Prevention Act of 1990 (H.R. 5372)*, Representatives T. Luken, and M. Sikorski, 1990.

11. Jin, S., "Deveoping Lead-Free Solder: A Challenge and Opportunity," *JOM The Journal of the Minerals, Metals, and Materials Society*, volume 45, number 7, July 1993.

12. Tu, K.N., and Thompson, R.D., "Kinetics of Interfacial Reaction in Bimetallic Cu-Sn Thin Films," *Acta Metallurgica*, volume 30, May 1982.

13. Parent, J.O.G., Chung, D.D.L., and Bernstein, I.M., "Effects of Intermetallic Formation at the Interface Between Copper and Lead-Tin Solder," *Journal of Materials Science*, volume 23, pp. 2564-2572, 1988.

14. Davis, P.E., Warwick, M.E., and Warwick, S.J., "Intermetallic Compound Growth and Solderability of Reflowed Tin and Tin-Lead Coatings," *Plating and Surface Finishing*, volume 70, August 1983.

15. Hagstrom, R.A., and Wild, R.N., in Proceedings of the Technical Programme, International NEPCON (National Electronic Packaging and Production Conference), Brighton, October 1969.

16. Muckett, S.J., Warwick, M.E., and Davis, P.E., *Plating and Surface Finishing*, volume 79, 1986.

17. Kang, S.K., and Ramachandran, V., "Growth Kinetics of Intermetallic Phases at the Liquid Sn and Solid Ni Interface," *Scripta Metallurgica*, volume 14, 1980.

18. Morris, J.W., Freer Goldstein, J.L., and Mei, Z., "Microstructure and Mechanical Properies of Sn-In and Sn-Bi Solders," *JOM The Journal of the Minerals, Metals, and Materials Society*, volume 45, number 7, July 1993.

19. Tomlinson, W.J., and Collier, I., "The Mechanical Properties and Microstructure of Copper and Brass Joints Soldered with Eutectic Tin-Bismuth Solder," *Journal of Materials Science*, volume 22, pp.1835-1839, 1987.

20. Pattanaik, S., and Raman, V., "Deformation and Fracture of Bismuth-Tin Eutectic Solder," *Materials Developments in Microelectronic Packaging*, ed. P.J. Singh, pp.251-257, ASM Publishing, 1991.

21. Freer, D.R., "Thermomechanical Fatigue in Solder Materials," *Solder Mechanics: A State of the Art Assessment*, ed. D.R. Frear, W.B. Jones, and K.R. Kinsman, pp. 191-237, TMS, 1991.

22. *Metals Handbook*, volume 13, American Sciety for Metals, 1985.

23. Klein Wassink, R.J., *Soldering in Electronics*, 2d ed., Electrochemical Publications LTD., 1989.

24. Smallman, R.E., *Modern Physical Metallurgy*, 4th ed., Butterworth and Company Publishers LTD., 1985

INITIAL DISTRIBUTION LIST

1. Defense Technical Information Center Cameron Station Alexandria, VA 22304-6145	2
2. Library, Code 0142 Naval Postgraduate School Monterey, CA 93943-5002	2
3. S. Mitra 143 Johnstone Dr. San Francisco, CA 94131	1
4. Professor J. Perkins, code ME/Pe Naval Postgraduate School Monterey, CA 93943-5000	1
5. Fred Vollweiler 965 Whitehawk Trail Lawrenceville, GA 30243	1